THE OPTIMISATION OF BAFFLE ARRANGEMENTS FOR MINIMAL SEDIMENT WASHOUT IN STANDARD STORMWATER SUMPS

By

Leshalen Paideya

Student No: 217003834

Submitted in fulfilment of the requirements for the degree of

Master of Science in Civil Engineering

College of Agriculture, Engineering and Science

School of Civil Engineering, Surveying and Construction

University of KwaZulu-Natal

Howard College Campus

Durban

2022

Supervisors: Prof. M Kumarasamy/Dr J Adu

As the candidate's Supervisor, I agree/do not agree to the submission of this thesis.

_____ _____

Prof. M. Kumarasamy Dr J. Adu

DECLARATION

I, Leshalen Paideya, declare that

1. The research reported in this thesis, except where otherwise indicated, is my original research.

2. This thesis has not been submitted for any degree or examination at any other university.

3. This thesis does not contain other persons' data, pictures, graphs or other information, unless specifically acknowledged as being sourced from other persons.

4. This thesis does not contain other persons' writing, unless specifically acknowledged as being sourced from other researchers. Where other written sources have been quoted, then:
    a. Their words have been re-written but the general information attributed to them has been referenced.
    b. Where their exact words have been used, then their writing has been placed in italics and inside quotation marks, and referenced.

5. This thesis does not contain text, graphics or tables copied and pasted from the Internet, unless specifically acknowledged, and the source being detailed in the thesis and in the References sections.

Signed

_____ 7 July 2022

Leshalen Paideya Date

ACKNOWLEDGEMENTS

First and foremost, thank you to my parents for all the love and support you have given me throughout the course of completing this dissertation and my tertiary education in its entirety. I am forever grateful for all you do for me and will always strive to make you proud.

Thank you to Prof. M.V. Kumarasamy and Dr J.T. Adu for their consistent guidance with this dissertation throughout the year.

Many thanks go out to Mr Logan Govender, Mr Lingis Pillay, Ms Fathima Ali and Mr Ishaan Ramlakhan for facilitating my work in the Fluid Mechanics and Environmental Engineering laboratories, especially in light of the COVID-19 pandemic.

Finally, thank you to my fellow colleagues and lab partners, Jiven Govender and Neekara Maharaj. I would not have been able to produce an investigation of this calibre without your support and assistance throughout the year.

ABSTRACT

Sediment in stormwater drainage systems is a matter of great concern due to its ability to collect within stormwater pipes to form blockages. Furthermore, sediments transport harmful pollutants, depositing them in stormwater discharge areas and disturbing the ecology of those areas. Standard stormwater sumps are a reliable and cost-effective solution to trap and retain sediment within stormwater drainage systems for manual removal. However, under high flowrate and fine sediment conditions, the effectiveness of standard sumps drastically decreases. A solution to this issue is the installation of baffles that can be retrofitted into the standard sump as a method of reducing flow velocities to allow sediments to settle to the sump bed.

An aspect of this solution, as equally important as sediment trapping, is the prevention of sediment washout. During a storm event, sediment previously trapped in a stormwater sump can be washed out before the routine cleaning period. Therefore, it is paramount to ensure that the baffle arrangement effectively prevents the resuspension and washout of sediment already present in a standard sump.

This dissertation investigates the use of baffle arrangements to minimise sediment washout in standard sumps and determine a baffle arrangement that will provide the best sediment retention results while remaining a feasible and practical solution in a real-world context.

Three baffle arrangements, consisting of a combination of solid and semi-porous baffle plates of varying dimensions placed in different orientations, were chosen for this investigation based on their previous success with sediment trapping. The primary methodology of this research compared the effectiveness of these baffle arrangements in minimising sediment washout by comparing them to a control setup with no baffles, using a simple mass-balance process. Additional experimentation involved using an Acoustic Doppler Velocimeter (ADV) to develop flow velocity fields to motivate the observations made in the mass-balance tests.

All baffle arrangements performed better than the control setup, with the least effective of the three designs improving sediment retention efficiency by 22% and the most effective by 71.5% under the worst-case condition. These results were then dimensionally analysed to determine the results of such testing under real-world conditions. The results of this analysis were also promising, with the best baffle arrangement achieving retained effluent concentrations of up to 0.4 kg/m^3 when calibrated for typical standard sump dimensions and peak flowrate.

TABLE OF CONTENTS

LIST OF FIGURES

LIST OF TABLES

LIST OF EQUATIONS

NOMENCLATURE

ADV - Acoustic Doppler Velocimeter

B1 - Baffle Arrangement 1

B2 - Baffle Arrangement 2

B3 - Baffle Arrangement 3

η - Sediment retention efficiency

C - Effluent sediment concentration

SG - Specific Gravity

ρ_w - Density of water

Pe - Péclet number

Fr - Froude number

Q - Discharge/flowrate

U_j - Inlet jet velocity

U_s - Sediment settling velocity

g - gravitational acceleration

1. INTRODUCTION

1.1. Motivation

Sediment in stormwater drainage systems is a matter of great concern from a fluid mechanics and environmental viewpoint. The accumulation of sediment in stormwater drainage can clog filters and block pipelines, thus causing significant strain in drainage systems (Quang *et al.*, 2022). Environmentally, sediment in stormwater runoff is known to transport pollutants in drainage systems. The sediments are also responsible for creating unfavourable living conditions for aquatic flora and fauna present at the discharge points of stormwater drainage systems (Ma and Zhu, 2014). For these reasons, the collection and removal of sediment in stormwater drainage systems is paramount for the proper functioning of stormwater drainage systems and the environment as a whole.

While conventional methods of actively removing sediment from stormwater drainage systems have been used in the past, these techniques are not preventative and are only conducted when hydraulic restrictions occur. Therefore, standard sumps are a favourable solution to this problem, as they use physical rather than chemical processes to remove sediment from the drainage system and require simple maintenance procedures. However, the effectiveness of a standard sump is extremely low under conditions with high flowrates and fine sediments. Therefore, introducing baffle plates into the standard sump is required for improved sediment collection.

An aspect of this solution, as equally important as sediment trapping, is the prevention of sediment washout. During a storm event, sediment previously trapped in a stormwater sump can be washed out before the routine cleaning period. Therefore, it is paramount to ensure that the baffle arrangement effectively prevents the resuspension and washout of sediment already present in a standard sump.

This dissertation investigates the use of baffle arrangements to minimise sediment washout in standard sumps and determine a baffle arrangement that will provide the best sediment retention results while remaining a feasible and practical solution in a real-world context.

1.2. Research Question

This work seeks to answer the following question: What standard sump baffle design will provide the most effective sediment retention and create minimal sediment resuspension under varying flowrate and sediment size conditions?

1.3. Research Aims

- Determine an effective baffle arrangement that will produce minimal sediment resuspension in stormwater standard sumps.
- Determine the effects of this baffle design under real-world conditions.

1.4. Research Objectives

- To evaluate sediment transport in stormwater drainage and the effects of retrofit baffle arrangements in standard stormwater sumps for possible improvements.
- To assess sediment retention efficiencies in comparison to a standard stormwater sump using select baffle configurations.
- To determine sediment transport behaviour in validation of the sediment retention experimentation for various baffle arrangements.
- Determine real-world conditions for these baffle efficiencies through dimensional analyses.

1.5. Scope of Research

This study considers the effectiveness of standard sumps with the assumption that sediment runoff is the only pollutant entering the standard sump. Variation in the sediment's chemical properties is limited, as sediment samples originating from a single area (Umgeni, Durban) are considered. The effectiveness of the standard sump's sediment retention is tested under non-uniform steady-state flow conditions. The study considers the washout of sediments with a shallow accumulation relative to the depth of the stormwater sump and does not consider scenarios where the accumulation of sediment reaches the depth of a baffle plate. Finally, the investigation of this study is conducted through laboratory testing instead of a practical stormwater drainage system. However, the results of these laboratory tests undergo a dimensional analysis to compare them to practical conditions.

1.6. Outline of the Dissertation

Chapter 1 outlines the basic background information on the research and the importance of pursuing this topic. Research aims and objectives have also been outlined.

Chapter 2 provides a critical review of available literature on sedimentation in stormwater drainage and previous experimental techniques for preventing sediment re-entrainment in stormwater drainage.

Chapter 3 details the methodological approach used to analyse sediment washout in stormwater standard sumps. The experimental apparatus, equipment and materials used during experimentation are presented, along with detailed explanations of the experimental procedures carried out.

Chapter 4 presents the results obtained from all experimental tests conducted. The sediment retention efficiencies of all sump configurations are discussed in detail, with attention to relations with flowrate, sediment grain sizes, influent sediment mass, scouring patterns and velocity flow fields.

Chapter 5 presents the conclusions derived from the investigation. In this chapter, the experimental results are provided and related to the research aims and objectives while answering the research question. Finally, recommendations for further research are provided.

2. LITERATURE REVIEW

2.1. Introduction

Sediment transport in urban stormwater drainage and its mitigations are complex topics that depend on various external (environmental, socio-economic) and internal (physical and fluid dynamic properties) factors. The following literature review serves to achieve a greater understanding of these factors. A critical analysis of research relating to sedimentation in urban stormwater, various mitigative processes (including standard sumps), sediment properties and the effects of baffles on sediment trapping and retention is performed in the review. Conclusions from the analysis of these factors can be drawn to produce a comprehensive experimental methodology.

2.2. Sediment transport in Urban Stormwater Drainage

Sediment can be defined as solid particles or debris transported by one of several fluid media, such as water, wind, glaciers, and waves, or found in deposits after transportation (Chien and Wan, 1999). The primary source of sediment particles originates from the weathering of rocks through mechanical or chemical processes. The most common natural occurrences of sediment transport are through rainfall events (Fondriest Environmental, 2022). As rainfall lands on embankments, a portion of the rainfall will be absorbed into the underlying soil. The excess portion of rainfall travels overland, where sediment particles in the topsoil are collected by the runoff and transported downhill (Fondriest Environmental, 2022). The sediment particles may vary in size and concentration based on the characteristics of the rainfall collecting the sediment, such as the rainfall intensity, peak discharge, rainfall depth and antecedent dry periods (Ma and Zhu, 2014).

In areas where the predominant landmass consists of natural features (such as rural areas and remote wilderness), the collection point of the stormwater runoff would be nearby water bodies such as rivers and streams. The vegetation of these areas naturally prevents excessive amounts of sediment from being transported into these catchment areas (Montakhab *et al.*, 2012). In urban areas, however, the lack of natural vegetation means there is no protection preventing large sediment deposits from being transported from embankments into urban stormwater drainage systems. In urban areas that are subject to high-intensity rainfall throughout the year, the effects of such excessive sedimentation would be highly detrimental to the stormwater drainage system (Quang *et al.*, 2022).

2.3. The effects of Sedimentation in Urban Stormwater Drainage

Sediment accumulation in stormwater drainage pipes narrows the cross-section of these pipes, subsequently increasing the Manning coefficient within the stormwater pipelines, thus disrupting stormwater flow (Quang *et al.*, 2022). Further consequences of this accumulation include eventual blockage and early surcharges, ultimately causing significant strain on the stormwater drainage system, which would be costly to rectify.

Environmentally, sediment runoff can absorb pollutants such as chemicals and heavy metals transported to the drainage systems via stormwater runoff (Ma and Zhu, 2014; Alam *et al.*, 2018). If the stormwater is discharged into streams, rivers, lakes and estuaries without treatment and eventually makes its way to the open sea, the contaminated sediment can endanger any aquatic flora and fauna it encounters (Armitage, 2007; Ma and Zhu, 2014).

During the *International Workshop on Origin, Occurrence and Behaviour of Sediments in Sewer Systems* (held in Belgium, 1991), one of the significant conclusions made was that the many problems relating to sewer sediments, such as washout of pollutants during storm overflows, reduction of hydraulic capacity, recurrent costs for cleaning sewerage lines and tanks, should be a fundamental consideration in the design and analysis of all urban stormwater drainage (Verbanck, Ashley and Bachoc, 1994).

From the two perspectives provided, one from a fluid dynamics viewpoint and the other from an environmental viewpoint, the following conclusions can be drawn. Firstly, implementing preliminary sediment removal systems is necessary to prevent the occurrence of any fluid dynamic-related incidents. Secondly, the collection and removal of sediment from stormwater drainage systems are paramount to the sustainability of the environment.

2.4. Conventional Methods of Sediment Trapping in Urban Stormwater Drainage

Conventional techniques used in removing sediments from stormwater drainage systems that do not require additional infrastructure include rodding, balling, flushing, poly pigs and bucket machines (Fan *et al.*, 2001). While these methods can effectively remove sediment from stormwater drainage, they are not regularly performed and are only utilised in the case of a blockage in the drainage system causing a hydraulic restriction (Fan *et al.*, 2001).

Therefore, preventative methods of sediment removal should be implemented, as these processes are passive and instantaneous and require only regular maintenance procedures. Furthermore,

preventative sediment removal methods would reduce the frequency of hydraulic restrictions to practically non-existent events.

2.5. The utilisation of Standard Stormwater Sumps for Sediment Trapping

A sump (also known as a catch basin) can be defined as a structure built at regular intervals throughout a stormwater drainage system to access and maintain the drainage system and create a space for joining multiple stormwater pipes (Howard, Stefan and Mohseni, 2010).

Sumps/catch basins may have multiple shapes and dimensions based on the requirements of the stormwater drainage system in which they are placed. Typically, sumps may be square or circular-based in shape. **Figure 2-1** and **Figure 2-2** provide two examples of sump designs. Sumps may be designed to connect to a stormwater drainage system directly from a surface drain (**Figure 2-1**) or as an intermediate catchment device between two or more stormwater drainage pipes (**Figure 2-2**).

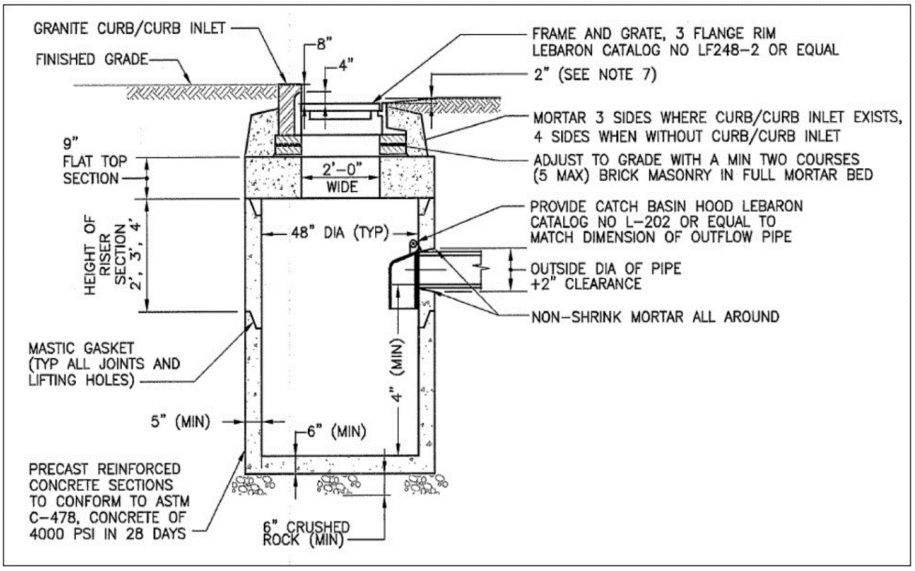

***Figure 2-1**: Stormwater sump detail (Commonwealth of Massachusetts, 2008)*

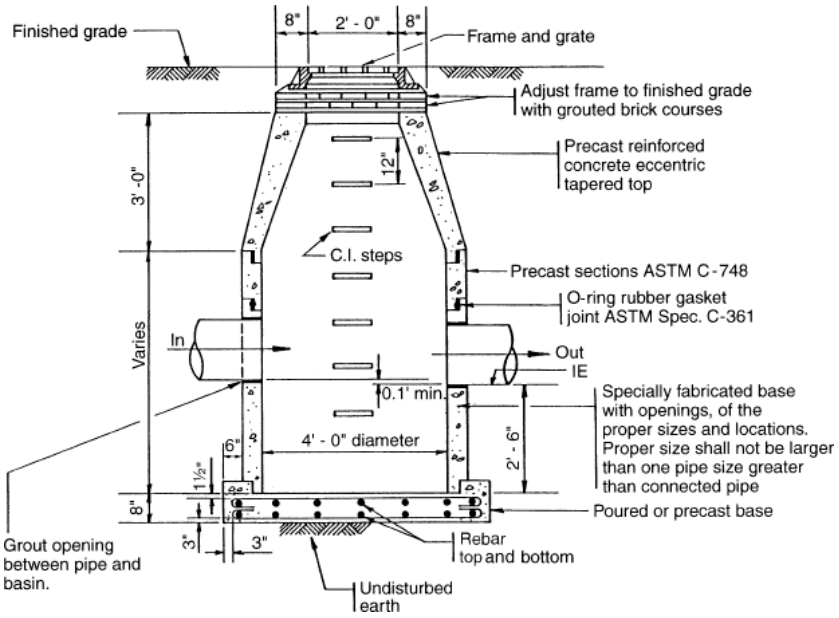

***Figure 2-2**: Stormwater sump detail (Frankel, 2012)*

A study conducted by Smith, Abumaizar and Skipwith in 2001 was one of the earliest investigations into stormwater drainage systems that highlighted the use of sumps as an alternative sediment trapping method (and subsequent stormwater purification) to detention basins (also known as retention ponds). This observation was the first step toward understanding stormwater sump potential for sediment trapping and removal purposes.

However, it was not until years later that the effectiveness of a standard sump for sediment removal and retention was analysed. One of the most prominent returns to the subject was a study conducted by Howard, Stefan and Mohseni (2010). In this study, tests were undertaken to evaluate the effectiveness of standard sumps for sediment capture and washout. The study used a single SAFL semi-porous retrofit baffle to increase the sump's sediment removal and retention effectiveness under higher flowrate conditions (Howard, Stefan and Mohseni, 2010).

Over the past decade, there have been further advancements to this study, with researchers (Howard *et al.*, 2012; Ma and Zhu, 2014) developing new baffle arrangements to improve the effectiveness of sediment trapping and retention.

Another critical study that tests baffle arrangement effectiveness is the works of Ma and Zhu (2014). They developed two multi-baffle arrangements consisting of both semi-porous and non-porous baffles to improve the effectiveness of sediment removal in a standard sump model. The results of this study were very successful.

2.6. Alternative Sediment Trapping Methods and their Comparison to Stormwater Sumps

2.6.1. Retention ponds

Historically, one of the most common forms of sediment removal structures is the sediment retention pond. Retention ponds have been a widely accepted infrastructure due to their effectiveness in trapping and retaining sediment in stormwater drainage systems.

However, various factors make retention ponds a far less viable option for removing sediment in stormwater drainage than standard sumps (Haris *et al.*, 2016). These factors are due to the sediment retention efficiency being dependent on the retention pond's volume, including area constraints brought about by constant urbanisation, high costs associated with the construction of the retention pond, and maintenance costs.

In contrast, the integration of stormwater sumps into stormwater drainage systems solves both problems by reducing the required space needed for sediment removal and retention and subsequently reducing the costs associated with sediment removal (Selbig *et al.*, 2016).

Furthermore, a study conducted by Selbig *et al.* (2016) noted a similar performance of standard sumps in sediment removal and retention compared to retention ponds. This study proved that similar levels of sediment capturing could be achieved using a smaller catchment area, making stormwater sumps a viable alternative to retention ponds.

2.6.2. Hydrodynamic separators

Hydrodynamic separators (also known as vortex grit chambers) are structures similar in shape to standard sumps but differing in their method of sediment removal. Sediments are collected in hydrodynamic separators through the separators' ability to produce vortex currents that pull the sediments and any other foreign contaminants to the chamber's floor (Pretorius, 2012).

These structures are known to be one of the most efficient methods of sediment removal in stormwater drainage systems but are more costly to construct and maintain than standard sumps. For this reason, the use of hydrodynamic separators is only implemented in areas with adverse pollution issues (Pretorius, 2012).

2.7. The Effectiveness of Standard Sumps on Typical Stormwater Waste

Thus far, it has been determined that standard stormwater sumps are suitable devices for sediment trapping and collection. However, the same cannot be said when considering stormwater waste holistically. Typical stormwater waste other than sediment runoff include general solid waste/litter and chemical waste (Armitage, 2007). While chemical waste can be disregarded at this early stage in the water recycling process (where the effluent water is still within the stormwater drainage system), the effects of litter cannot be ignored, as it could reduce the effectiveness of sediment trapping techniques or the functioning of a stormwater drainage system altogether (Alam *et al.*, 2018). Within a stormwater sump, the accumulation of litter would reduce the available volume for sediment trapping and, with the addition of baffle plates or in excessive amounts, could create a hydraulic restriction within the stormwater drainage system (Alam *et al.*, 2018). Therefore, it is best to consider the implementation of standard sumps within a stormwater drainage system when mitigative procedures are already in place to remove general solid waste.

Studies have been conducted in which standard sumps were installed as temporary sediment catchment devices at construction sites. An investigation conducted by Basham, Zech and Donald (2019) evaluated the use of stormwater sumps installed with different Catch Basin Inserts (CBIs) for their potential use as post-construction stormwater devices for projects undertaken by the Ohio Department of Transportation. This investigation concluded that the most effective CBI could produce sufficient sediment retention efficiencies, making it a viable choice for post-construction sediment collection (Basham, Zech and Donald, 2019). These findings indicate that stormwater sumps may also take on a specialised function for construction sites.

2.8. The implementation of Baffles into Standard Stormwater Sumps

The use of standard sumps is a favourable solution to the problem of sediment removal in stormwater drainage systems. However, tests conducted by Howard *et al.* (2012) showed that with the increase in the magnitude of stormwater discharge, the effectiveness of a standalone stormwater sump decreases significantly. For this reason, the implementation of baffles into the standard sump is required to mitigate this drastic change in sediment collection and retention performance.

Baffles are solid structures that create a partition in a standard sump, subsequently forcing stormwater to flow through a longer path. This increased flow path decreases the flow velocity of the stormwater, thus allowing sediment transported in the stormwater to settle in the sump bed.

Baffle designs are specifically designed to suit the environment and functioning of the stormwater drainage system housing the sump/catch basin. A single-chamber standard sump housing a single

non-porous baffle would be sufficient for acceptable sediment collection and retention in an environment with lower peak flood rates and low sediment runoff (Farjood, Melville and Shamseldin, 2015). In contrast, an environment having higher peak flood rates and carrying an assortment of pollutants such as high amounts of sediment runoff and other particulate waste would require a more complex stormwater sump consisting of multiple baffle-divided chambers (and in extremely adverse conditions, the addition of a vortex grit chamber) (Pretorius, 2012).

2.9. Sediment Characteristics and their Effects on Sediment Trapping Efficiency

Three sediment characteristics concerning the effectiveness of sediment trapping will be discussed: critical shear stress, the concentration of trapped sediment within the sump, and turbulence.

2.9.1. Critical Shear Stress

In a study conducted by Glasbergen *et al.* (2014), tests comparing the critical shear stress of various sediment samples to the concentration of suspended sediment over time were conducted. The results of this study found that finer sediments with higher shear stresses settled much slower than coarse sediments with lower shear stresses due to the stronger shear forces (in the form of buoyancy forces and drag forces) resisting the gravitational forces acting on the sediment particles (Glasbergen *et al.*, 2014). This phenomenon is shown in **Figure 2-3**:

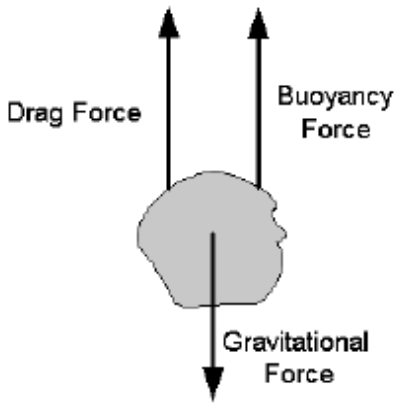

***Figure 2-3**: Forces acting on a suspended sediment particle (Dueñas Díez et al., 2002)*

2.9.2. Concentration of trapped sediment

The constant addition of sediment settling in a stormwater sump over a period of time may result in the occurrence of one of two scenarios. In the first scenario, the cohesive forces between the settled sediment particles may produce a higher resistance to resuspension and washout. Alternatively, the sediment may be likely to resuspend due to the reduced depth of overlying water and may produce surges in stormwater inflow for future storm events. In the case of the second scenario, the frequency of maintenance of standard sumps should be determined to prevent such an incidence from occurring.

2.9.3. Turbulent flow

Turbulence can be characterised as an irregular, diffusive, unsteady flow within a fluid body. During turbulent flows, fluid particles vary in velocity, thus creating a "mixing" within the fluid and the formation of eddies (whirling bodies within a fluid) (Davidson, 2015).

Because the analysis of turbulent flow in larger bodies of water is too complex to solve using simple equations, its analysis is mainly conducted using experimental or numerical methods or a combination of the two methods (Faram and Harwood, 2002).

2.10. Characteristics of sediment transport

Based on sediment size and flow characteristics, there are three basic methods of sediment transport in a fluid body, namely rolling/skidding, saltation (lifting and resettling above the flow bed), and suspension (Sherman, Davis and Namikas, 2013).

For optimal sediment retention in standard stormwater sumps, bedload transport, such as rolling/skidding and saltation, are acceptable methods of sediment transport, while suspension is unfavourable as it allows the sediment particles to be carried out of the sump by the flowing current.

Relationships between sediment sizes and their threshold points between sedimentation and transportation have been developed in the form of Hjulström's Curve (as a function of flow velocity) (Sherman, Davis and Namikas, 2013). This curve is provided in **Figure 2-4**.

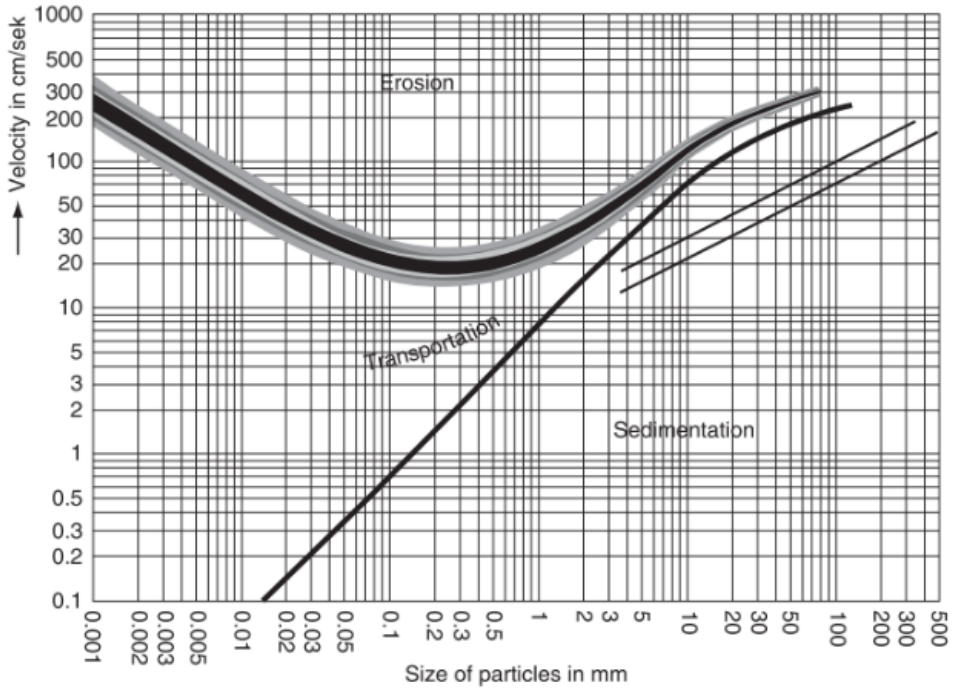

***Figure 2-4**: Hjulström's Curve (Sherman, Davis and Namikas, 2013)*

The use and application of Hjulström's Curve may be used to determine the critical flow velocities required for re-entrainment in each baffle arrangement. Therefore, this dissertation will relate to the effectiveness of the standard sump with the implementation of baffle arrangements in relation to Hjulström's Curve in order to obtain a better understanding of sediment transport behaviour within a standard sump.

2.11. Methods of Testing the Effectiveness of Sediment Retention Techniques

Previous research has defined two primary forms of testing for the effectiveness of sediment removal in stormwater drainage systems, namely testing by numerical methods and testing by experimental methods (Faram and Harwood, 2002; Howard *et al.*, 2012). Researchers (Howard *et al.*, 2012; Ma and Zhu, 2014) have used a combination of the two methods to ensure that the results obtained were of the highest possible level of accuracy.

2.11.1. Numerical Methods

A study conducted by Faram and Harwood (2002) developed a numerical method relating to sediment retention techniques. Their methodology included Lagrange particle tracking

approaches paired with fluid flow simulation software to analyse different sediment removal processes.

Faram's and Harwood's (2002) testing method works primarily with software over physical experimentation, which is a less labour-intensive testing method but can produce inaccurate results if the amount of sample data collected is not sufficient for testing.

2.11.2. Experimental Methods

According to the methodology of testing by Howard, Stefan and Mohseni (2010), a mass-balance approach was considered by introducing a known mass of sediment into the drainage system, simulating a storm event, and then collecting all sediment remaining in the sump for drying and weighing to compare to the original value. The efficiency of the stormwater sump was then calculated using **Equation 2-1** (Howard, Stefan and Mohseni, 2010):

$$\eta = \frac{C_{in} - C_{out}}{C_{in}} \qquad \textit{(Equation 2-1)}$$

Where **η** refers to the sediment trapping efficiency, $\mathbf{C_{in}}$ is the influent sediment concentration, and $\mathbf{C_{out}}$ is the effluent concentration, where $C_{in} - C_{out}$ is the concentration of sediment trapped in the standard sump (Howard *et al.*, 2012).

In this method, the measurement of stormwater concentration remaining in the sump is preferred over the comparison of influent and effluent stormwater concentrations, as this comparison is known to be unreliable when analysing stormwater concentrations with larger sediment particles (Howard, Stefan and Mohseni, 2010).

The effectiveness of the baffle arrangement under real-world conditions is determined using the method developed by Howard *et al.* (2012) will be utilised that derives washout efficiency as a function of sediment characteristics, the sump dimensions, stormwater flowrate and sump inlet velocity. This "Washout Function" is expressed as **Equation 2-2** (Howard *et al.*, 2012).

In this equation, the effluent sediment concentration $\boldsymbol{C}$ (kg/m^3), specific gravity $\boldsymbol{SG}$ and density of water $\boldsymbol{\rho_w}$ (kg/m^3) are calculated as a function of the dimensionless Péclet and Froude numbers (Howard *et al.*, 2012). The Péclet number can be defined as a dimensionless parameter relating the flow characteristics of a moving body as a ration of its thermal conductivity (Shires, 2011). Similarly, the Froude number is a dimensionless parameter relating to the physical properties of a moving body and can be defined as the ratio of inertial force to gravitational force (Rapp, 2016).

The equations for these dimensionless parameters are provided as **Equation 2-3** and **Equation 2-4**.

In **Equation 2-3**, the Péclet number ***Pe*** is expressed as a function of sediment settling velocity $\boldsymbol{U_s}$ (m/s), sump depth $\boldsymbol{h}$ (m), sump length $\boldsymbol{L}$ (m) and stormwater discharge $\boldsymbol{Q}$ (m^3/s). **Equation 2-4** expresses the Froude number ***Fr*** as a function of the stormwater jet velocity $\boldsymbol{U_j}$ (m/s), gravitational acceleration $\boldsymbol{g}$ (m/s^2) and sump length $\boldsymbol{L}$ (m) (Howard *et al.*, 2012).

$$\frac{C(SG-1)}{\rho_w SG} = f\left(\frac{Pe}{Fr^2}\right) \qquad \textit{(Equation 2-2)}$$

$$Pe = \frac{U_s hL}{Q} \qquad \textit{(Equation 2-3)}$$

$$Fr = \sqrt{\frac{{U_j}^2}{gL}} \qquad \textit{(Equation 2-4)}$$

2.12. Acoustic Doppler Velocimeters as Stormwater flow field modelling devices

Testing the effectiveness of various baffle arrangements for sediment retention would be futile if a greater understanding of sediment transport was not attained. Without this understanding, the baffle arrangements cannot be improved in order to obtain the desired optimal results. Therefore, understanding the interactions amongst sediment particles within the stormwater sump can be seen as a complementary procedure to testing the sediment retention efficiencies of every stormwater sump configuration, as it will provide further insight into the improvements that can be made to the baffle arrangements.

An effective method of measuring such interactions would be by using an Acoustic Doppler Velocimeter (ADV). An ADV is a device typically used in hydraulic laboratories or on-site to measure turbulence and flow velocities within flumes and physical models (Nortek, 2021). The principle of the device's function makes use of the Doppler Effect, which is a phenomenon where the frequency of sound waves propagating off an object changes as the object moves towards/away from the observer or vice versa (Nortek, 2021).

The ADV operates by transmitting pairs of sound pulses into the water column. The pulses reflect off tracers, such as suspended sediment particles, that travel at the same average velocity as the water and return to the ADV. Once detected by the ADV, the pulses are processed to determine the relative change in position of the tracer (Nortek, 2021). **Figure 2-5** provides a representation of this process:

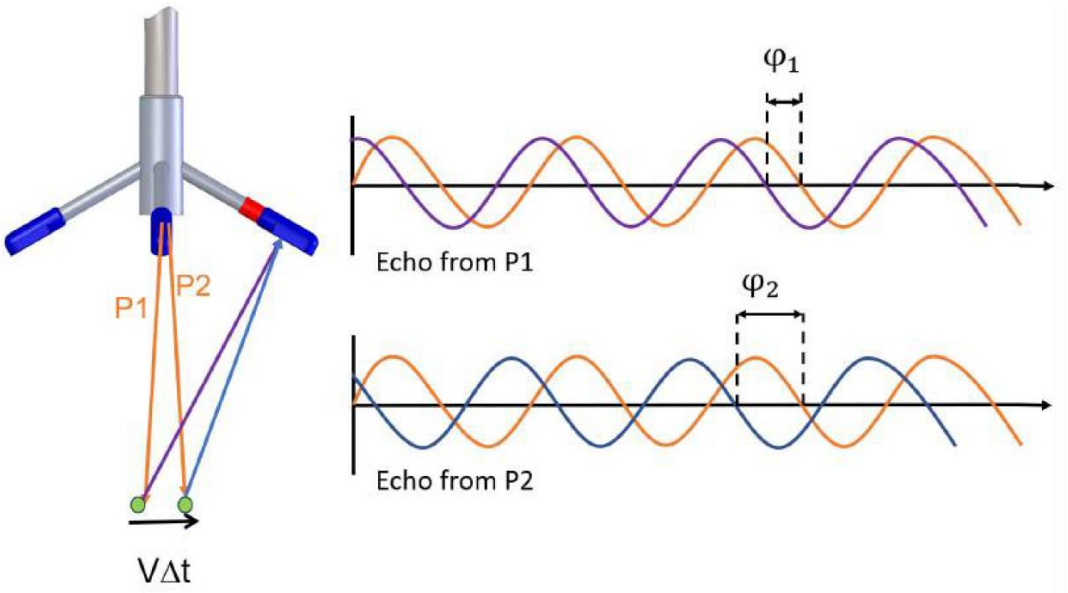

***Figure 2-5**: ADV's use of the Doppler Effect to determine flow velocities (Nortek, 2021)*

As shown in **Figure 2-5**, a tracer's velocity is determined by processing the change in phase between the two pulses reflected off the tracer as it travels in the direction of flow. The velocity of the tracer is calculated using **Equation 2-5** (Nortek, 2021):

$$V = \frac{\Delta\varphi C}{4\pi F_{source}\,\Delta t} \qquad \textit{(Equation 2-5)}$$

Where $\boldsymbol{V}$ represents the flow velocity (m/s), $\boldsymbol{\Delta\varphi}$ represents the difference in phase between the two pulses (m), $\boldsymbol{C}$ represents the speed of sound in the liquid (m/s), $\boldsymbol{F_{source}}$ represents the transmitted frequency (Hz), and $\boldsymbol{\Delta t}$ represents the difference in time between the two pulses (s).

Researchers (Asgharzadeh, Firoozabadi and Afshin, 2011; Howard *et al.*, 2011; Shahrokhi *et al.*, 2013; Sahin, Ozturk and Aydogan, 2020) have made use of ADVs to quantify suspended sediment

concentrations in a laboratory setting, making them ideal instruments for performing similar tests in a stormwater sump model.

During this investigation, ADV flow velocity measurements will be used to determine velocity flow fields within each sump configuration to validate the sediment retention efficiencies calculated for each configuration.

2.13. Trends in the Effectiveness of Baffle Arrangements in Standard Sumps

Current trends in the effectiveness of baffle arrangements will be discussed in terms of baffle shape, baffle angle and baffle position.

2.13.1. Baffle Shape

In a study by Nighman and Harbor (1997), various observations were made regarding the positioning of baffles and their effect on the velocity and flow pattern of stormwater travelling through a catchment basin. The report noted three possible solutions to slowing the inlet velocity of the catchment basin. One of these methods was to position a non-porous baffle vertically, spanning the width of the basin, thus forcing the flow of water over the baffle. The second method proffered in the study was to place a non-porous baffle vertically, but unlike the first option, have this baffle spanning from the basin's floor to the water's surface, thus forcing the flow of water from the inlet to travel to the left and right of the baffle. The third solution largely mirrored the second solution insofar as it related to the positioning of the non-porous baffle but differed in the baffle's shape. The third option's shape consists of 45° angles from the centre of the inlet on both sides, thus creating a "V-profile".

From the three designs analysed, it could be perceived that the first design would be the most effective in reducing the velocity of stormwater in a standard sump, thus increasing the amount of sediment settling in the sump. This assumption can be explained by the use and application of Bernoulli's Equation (**Equation 2-6**). Because the flow of water can only be directed above the baffle, the elevation head of the stormwater flow would increase, thus decreasing the velocity head and allowing for the settlement of sediments.

$$P_1 + \frac{1}{2}\rho v_1^2 + \rho g h_1 = P_2 + \frac{1}{2}\rho v_2^2 + \rho g h_2 \qquad \textit{(Equation 2-6)}$$

2.13.2. Baffle Angle

Nighman and Harbor (1997) noted the importance of positioning baffles to alter the flow patterns of water entering a catchment basin. One of the most efficient applications of positioning baffles would be to angle a non-porous baffle at a decline towards the catchment outlet, thus creating a "bottleneck" effect on the flow of water travelling upwards towards the outlet. This bottleneck causes the water to circulate at the bottom of the basin, creating ample opportunity for suspended sediment to settle at the bottom of the basin (Nighman and Harbor, 1997).

2.13.3. Baffle Position

Farjood, Melville and Shamseldin (2015) conducted a test to determine the effectiveness of a single baffle at various positions relative to the inlet pipe of a sediment retention pond. The study showed that the baffle arrangement with the single baffle placed closest to the inlet pipe provided the most effective sediment retention compared to arrangements with a single baffle placed further away from the inlet (Farjood, Melville and Shamseldin, 2015).

The reason for this increased effectiveness was due to the observation that the baffle closest to the retention pond inlet produced the strongest recirculation current compared to the other arrangements, thus allowing the majority of the sediment flowing through the retention pond to continuously cycle between the inlet and the baffle until finally settling (Farjood, Melville and Shamseldin, 2015). In contrast, the baffles placed further away from the inlet pipe produced lower velocities at the bottom of the baffle and a "dead zone" between the inlet and the baffle, thus allowing more of the sediment to flow over the baffle due to higher velocities above the baffle (Farjood, Melville and Shamseldin, 2015).

Although the dimensions of a standard sump drastically differ from that of a retention pond (greater depth, shorter length and width), the results of this study can be replicated using a combination of non-porous and semi-porous baffles to create "chambers" in a standard sump. These chambers could produce strong recirculation currents that yield similar sediment retention results to those produced by Farjood, Melville and Shamseldin (2015). This concept was replicated in the study conducted by Ma and Zhu (2014), using two originally designed baffle arrangements. While the results of this study were promising, the baffle arrangements used have the potential for further optimisation.

Throughout this review, the most prominent studies noted on the use of baffles in standard stormwater sumps have been the studies of Howard *et al.* (2011) and Ma and Zhu (2014). While

these studies showed notable increases in stormwater trapping and retention, they were limited by baffle arrangements that were not optimised in functionality. The SAFL baffle design used by Howard *et al.*, (2011) consists of a single semi-porous baffle, which allows for improvements with the addition of more baffles. In contrast, the baffle arrangements designed by Ma and Zhu (2014) consist of multiple baffles, which is sub-optimal from a fabrication and maintenance point of view. This dissertation aims to optimise these conditions by determining an optimal baffle arrangement that provides maximum sediment retention while remaining simplistic in design.

For the purpose of this dissertation, a standard sump model housing different baffle arrangements; consisting of combinations of semi-porous and non-porous baffles will be used. The reason for this choice would be to develop the most cost-effective design that also has not been "over-designed" for the conditions the standard sump will encounter, as the stormwater will only carry suspended sediment.

Another factor that will be considered is the convenience of the baffle arrangement for the purpose of cleaning and maintenance of the standard sump. Accordingly, the advantages of an ideal baffle arrangement will be twofold: it should provide effective sediment trapping and retention properties while also being accessible for municipal workers to completely remove the trapped sediment and perform regular maintenance procedures on the sump.

2.14. Conclusion

In this literature review, the main topics regarding the removal and retention of sediment in stormwater drainage systems with the use of baffle arrangements in a standard sump have been discussed. From the reviewed literature, the following significant conclusions can be drawn:

- Baffle arrangements in a stormwater sump should be considered only when sediment or other particulate matter is the only solid waste within a stormwater drainage system.
- Simple mass-balance testing is the most reliable form of testing for sediment washout.
- Considerations for the optimal amount of sediment allowable in a standard sump before excessive washout occurs should be considered during the testing of the baffle arrangements.
- The design should incorporate chambers within the standard sump for recirculation currents of stormwater to occur, as this will develop a highly effective baffle arrangement to produce minimal sediment washout.
- The designed baffle arrangements should incorporate oblique baffles to improve the strength of recirculation currents produced in the sump.

3. METHODOLOGY

3.1. Introduction

The following methodology discusses the methodological approach, experimental apparatus, materials, and procedures utilised for the analysis of several baffle arrangements in their ability to optimise sediment washout in a standard sump. The primary forms of analysis include modelled mass-balance testing, the dimensional analysis of the results of this testing and flow field analyses of the baffle arrangements within a standard sump model.

3.2. Methodological Approach

The approach taken to determine the most effective baffle arrangement for optimal sediment retention was undertaken in three parts. Firstly, the proposed baffle arrangement designs were installed in a model stormwater drainage system, where quantitative sediment mass-balance experimentation was undertaken in comparison to a control model without a baffle arrangement. Secondly, the flow fields of the control model and baffle arrangements were measured and plotted to provide further insight into the results of the mass-balance testing. Finally, the results of the mass-balance testing underwent a scaling analysis to predict the effectiveness of the baffle arrangements in a practical setting.

For this dissertation, a similar methodological approach to Ma and Zhu (2014) (mentioned in **2.5** and **2.13.3**) will be adopted, in the sense that the experimental model will be tested as a square-based sump tank connected to the stormwater drainage system as an intermediate collection device.

3.3. Limitations & Uncertainties

3.3.1. Sediment sample sizes

The sediment samples chosen for experimentation were limited to a range of 75 – 300 μm. This limitation was validated by comparing the chosen range to sediment samples collected near stormwater drainage inlets.

3.3.2. Head losses

The stormwater drainage model is operated on a closed circuit; therefore, the head losses produced across the model sump were primarily dependent on the flowrate set by the pumps producing the flow rather than the effects of any sump configuration. This circumstance consequently rules out the use of head losses as a viable indicator of the different sump configurations' effectiveness. To overcome this limitation, an ADV was used to determine the changes in velocity head at multiple points within the model sump as opposed to measuring the net head loss between the sump inlet and outlet.

In a practical setting, as stormwater passes through the standard sump, each configuration will produce a distinguishable head loss when compared at constant flow conditions. Therefore, disregarding the head losses caused by each baffle arrangement introduced a margin of error when determining the effectiveness of each arrangement. This margin, however, was shown to be small enough to clearly distinguish the differences in effectiveness amongst all the sump configurations.

3.3.3. Mass-balance procedures

While the procedure conducted for the mass-balance tests provided definitive results, these results may not have been as accurate as possible. This issue stems from the use of petri dishes for placing sediment samples within the model sump and transporting sediment out of the sump for weighing. These petri dishes were lipped around their edges, thus introducing slight shear resistances (and ultimately acting as miniature baffles) as water flowed over them. For this reason, the results produced by these experiments may be slightly overstated. However, much consideration was taken in this regard; therefore, petri dishes with edges no taller than 5 mm were used, thereby reducing the magnitude of shear resistances produced by the lips to possibly negligible values.

Furthermore, retained sediment could have been displaced during the transportation of the petri dishes out of the model sump. Much care was taken to prevent this from happening and based on the results of experimentation, any error encountered was minimal as the results of each sump configuration follow trends with very few outliers.

3.3.4. Use of ADV

The use of the ADV for capturing flow data was limited to the area available to manoeuvre. This made the baffle arrangements with such restrictions difficult to interpret flow interactions and provide holistic reasoning for the sediment retention efficiencies produced by those arrangements.

The areas captured were, however, sufficient enough to create a general sense of the flow field as these were larger areas where turbulent flow and sediment uplift was more likely to occur.

3.4. Experimental Apparatus

3.4.1. Stormwater Sump Model

The setup used in these experiments is located in the Fluid Mechanics laboratory of the Centenary Building, Howard College campus. This model is a closed-circuit pump system consisting of three plexiglass tanks which each represent an element of the stormwater drainage system, being the stormwater supply, a standard sump and stormwater collection, respectively. The three tanks are connected with 71.5 mm plexiglass pipes. The collection and supply tanks are joined by two identical 650 W pumps connected to the setup in parallel. A schematic of the sump model and its actual image are provided in **Figure 3-1** and **Figure 3-2**, respectively:

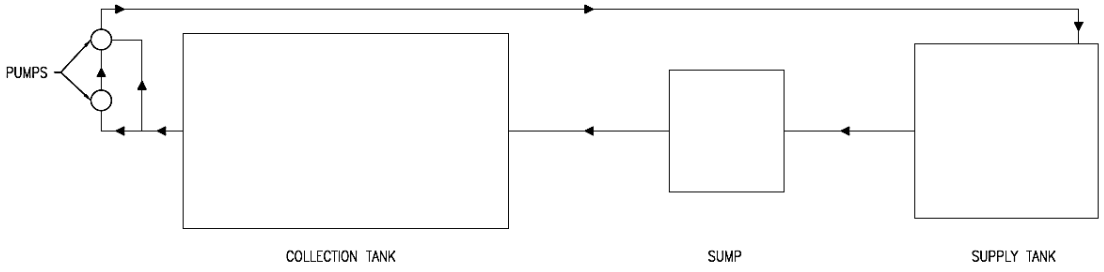

***Figure 3-1**: Schematic of experimental setup*

***Figure 3-2**: Stormwater sump model in Fluid Mechanics laboratory*

The reason for implementing three tanks rather than joining the pumps directly to the sump tank was to ensure steady flow between the pumps and the sump tank. Another measure implemented to ensure steady flow was the placement of the inlet pipe joining the pump to the supply tank at the bottom of the tank to reduce flow fluctuations at the water surface.

The dimensions of the model sump tank are provided in **Figure 3-3**:

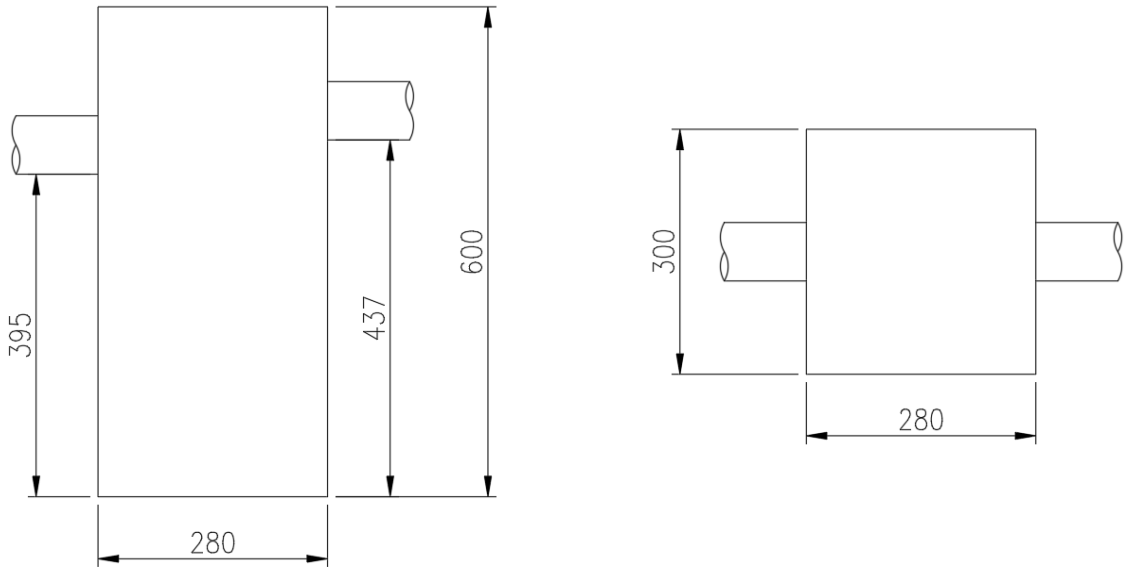

***Figure 3-3**: Model sump tank dimensions*

3.4.2. Baffle Arrangements

Three baffle arrangements were used for these experiments. The baffle plates were made of plexiglass and lined with foam sealing tape to secure the baffles to the model sump and ensure a watertight seal between the sump and the baffles. All designs were recommended due to previous success (Badge, 2019) when testing their effectiveness for sediment trapping in the standard sump.

Baffle Arrangement 1 (B1) consists of two solid baffles: a vertical 200 mm long baffle parallel to the sump inlet and an oblique 300 mm long baffle angled at 60° to the horizontal, towards the sump outlet, shown in **Figure 3-4**.

This baffle arrangement makes use of the concept observed by Nighman and Harbor (1997), where an angled baffle produces a “bottlenecked” flow, thus leading to lower flowrates at the bottleneck and prolonged stormwater recirculation, creating an extended period for sediment settling. The placement of an angled baffle at the inlet of the sump also mimics the designs used by Ma and Zhu (2014).

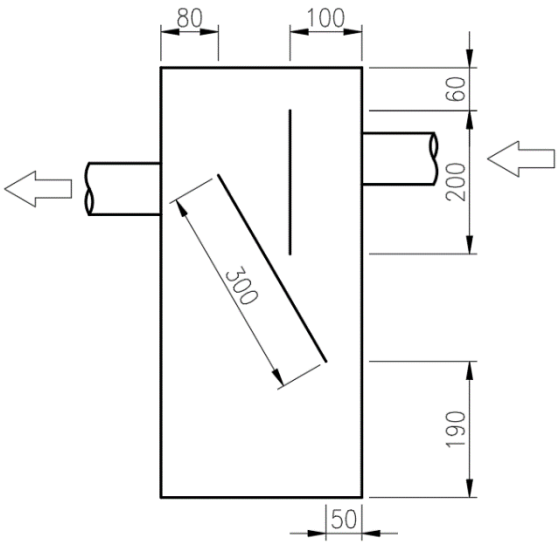

***Figure 3-4**: Baffle Arrangement 1*

Baffle Arrangement 2 (B2) consists of three baffles: two solid vertical baffles (200 mm parallel to the sump inlet and 300 mm below the sump outlet) joined by a horizontal 100 mm semi-porous baffle (**Figure 3-5**).

This arrangement provides two flow paths for the stormwater to follow to the sump outlet, either below the 300 mm vertical baffle or through the semi-porous baffle. Both flow paths produce energy losses for the stormwater, thus allowing any resuspended sediment to settle.

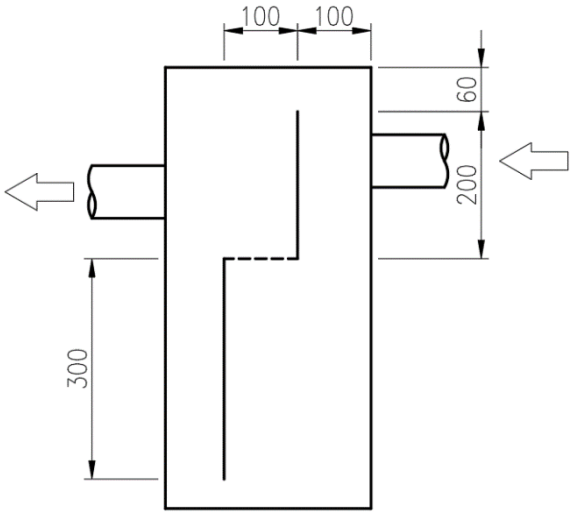

***Figure 3-5**: Baffle Arrangement 2*

Baffle Arrangement 3 (B3) (**Figure 3-6**) is designed similarly to B2, with the significant differences being that the 300 mm vertical baffle is replaced with a 400 mm baffle that stands flush with the sump bed, and the semi-porous baffle has been rotated vertically to sit on top of the 400 mm baffle.

This arrangement uses the concept observed by Nighman and Harbor (1997), where stormwater flow is forced over a solid baffle to reduce the velocity head of the flow, allowing sediment to settle before travelling to the sump outlet. This concept is paired with using a semi-porous baffle to further reduce flow velocities.

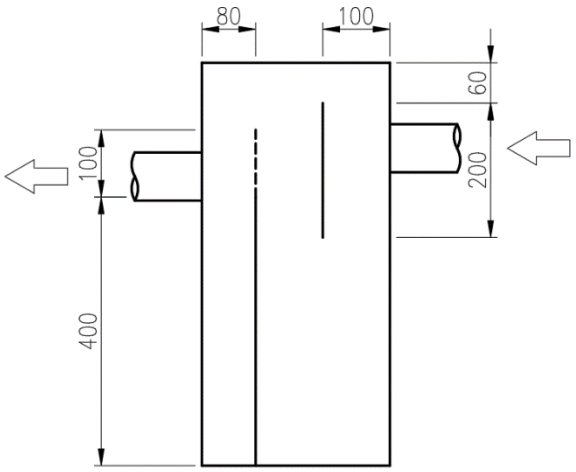

***Figure 3-6**: Baffle Arrangement 3*

3.5. Materials and Methods

3.5.1. Sediment samples

Three sand samples of varying grades (coarse, medium and fine sediment), uniformly graded by dry sieve processing, were used in these experiments. The rationale behind the selection of these sand samples was to provide a fair analysis by observing the sump efficiency with a range of sediment sizes. The grain sizes of each sample are as shown in **Table 3-1**:

***Table 3-1**: Grain sizes of sediment samples*

Sample Type	Grain size (µm)
Fine sediment	75 – 106
Medium sediment	106 – 150
Coarse sediment	150 – 300

The sediment samples were tested in varying mass quantities of 50g, 100g and 150g. This procedure aimed to determine an optimal sediment concentration in the model sump for maximum effectiveness in each sump configuration.

Additional sediment characteristics can be found in **Table A-2** of **APPENDIX A:**.

3.5.2. Validation of sediment samples

Sediment samples were collected from two stormwater inlets in Berea, Durban. The sediment grading results of these two samples were determined using dry sieve analysis. Afterwards, these results were averaged and are displayed in the Particle Size Distribution Curve, shown in **Figure 3-7**. The distribution curve is skewed to the left, indicating that these samples mainly consisted of fine sand to silty sediment particles. The most considerable proportion of sediment belonged to the 425 – 300 µm grain size range. However, these sediment grains would undergo physical erosion within a stormwater drainage system and become considerably smaller. Therefore, the sediment size ranges chosen for experimentation (300 – 75 µm) are within range of the typical sediment sizes found within a stormwater drainage system.

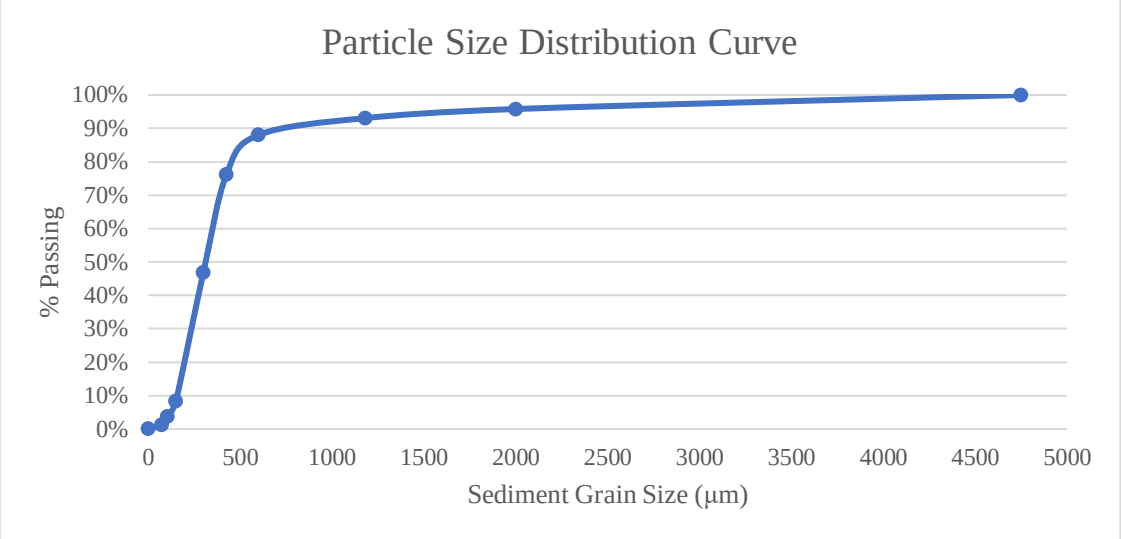

***Figure 3-7**: Sediment grading curve for typical stormwater sediment samples*

3.5.3. Sediment placement and transport

Four 100 mm diameter petri dishes were placed on the base of the sump tank to act as a medium for transporting sediment samples into and out of the sump.

3.5.4. Sediment Drying

To save time from drying substantial amounts of excess water from the sediment samples after testing, a vacuum pump is used to draw excess water from the sediment samples before oven drying.

The setup consists of an Erlenmeyer flask connected to a 2.4 bar pump. A porous stone was fitted to the top of the flask, and filter paper was placed over it to prevent any sediment from passing through and prevent the porous stone from becoming clogged with sediment. The setup is shown in **Figure 3-8** below:

***Figure 3-8**: Vacuum drying apparatus*

Beakers were used to transfer the wet sediment from the petri dishes to the vacuum pump. After draining the sediment, the samples were placed in an oven set to 70°C for 16 hours to remove all excess moisture before weighing.

3.5.5. Sediment Weighing

To determine the sediment washout mass, all sediment samples were weighed using a mass scale accurate to 0.1 mg before and after testing.

3.6. Flowrate Measurement

3.6.1. "Jug Method"

A measuring jug was placed under the sump outlet pipe and was allowed to fill for a specified period to determine the magnitude of low steady-state flow rates in the experimental setup. The flowrate was determined using a basic calculation, as seen in **Equation 3-1**.

$$Q = \frac{V_{water\ in\ jug}}{\Delta t} \qquad \textit{(Equation 3-1)}$$

In this equation, ***Q*** represents the calculated flowrate (l/s), ***V*** represents the volume of water present in the jug (l), and ***Δt*** represents the chosen measurement period (s).

3.6.2. Empirical Methods

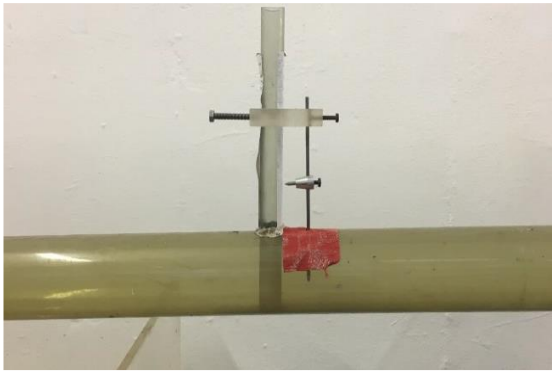

***Figure 3-9**: Cylindrical obstruction used in the sump model*

For higher steady flowrates, where the use of a jug to measure discharge would be impractical, Samani's (2017) method of flow measurements for circular flumes was employed. This method makes use of a cylindrical obstruction present in the sump outlet pipe of the experimental setup, as shown in **Figure 3-9**.

This obstruction induced a subcritical flow at its upstream end, which was measured and used in the following equation:

$$Q = aB_c{}^{2.5} g^{0.5} \left(\frac{H}{B_c}\right)^b \qquad \textit{(Equation 3-2)}$$

In **Equation 3-2**,$\boldsymbol{Q}$ represents the discharge (m^3/s), $\boldsymbol{B_c}$ represents the cross-sectional flow width at the water's surface (m), $\boldsymbol{g}$ represents gravitational acceleration (m/s^2), and $\boldsymbol{H}$ represents flow depth (m) (Samani, 2017). A schematic displaying the cylindrical obstruction within the pipeline is provided in **Figure 3-10**:

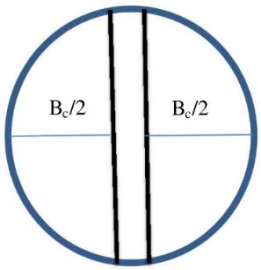

***Figure 3-10**: Cross-section of circular flume containing cylindrical obstruction (Samani, 2017)*

Variables $\boldsymbol{a}$ and $\boldsymbol{b}$ are calibration constants specific to the setup used for experimentation. These constants had been predetermined through tests conducted and found to equate to 0.57 and 2.04, respectively.

3.7. Washout Mass-Balance Experiments

Before each test could commence, the following preliminary procedures were conducted:

- All tanks were thoroughly cleaned to prevent contamination of the test samples.
- The supply tank was filled with water and allowed to spill into the sump and collection tank successively until all tanks had been filled to the desired depth. These depths were kept constant for all experiments. The tanks were filled to a standardised total volume of 180 l for every test.
- The pump inlet valve was opened, and the pumps were turned on and adjusted to the desired flowrate using the pump outlet valve and verified by using the obstruction method.
- After the flowrate was adjusted, the pumps were turned off, the pump inlet closed to prevent backflow, and the water levels of each tank were allowed to stabilise before starting the experiment.
- Following the completion of all the preliminary procedures, a sediment sample was weighed to a mass of 50 g using the mass scale.
- The mass of the watch glass and filter paper to be used later in the experiment was also weighed and recorded.

- After weighing, the sample was saturated by adding increments of water to it until a pasty texture was acquired. This procedure prevented the sample from clumping and instantaneously suspending (due to air pockets between sediment particles) when introduced to the water in the sump tank.
- After saturation, the samples were placed in four Petri dishes and positioned in the sump tank.

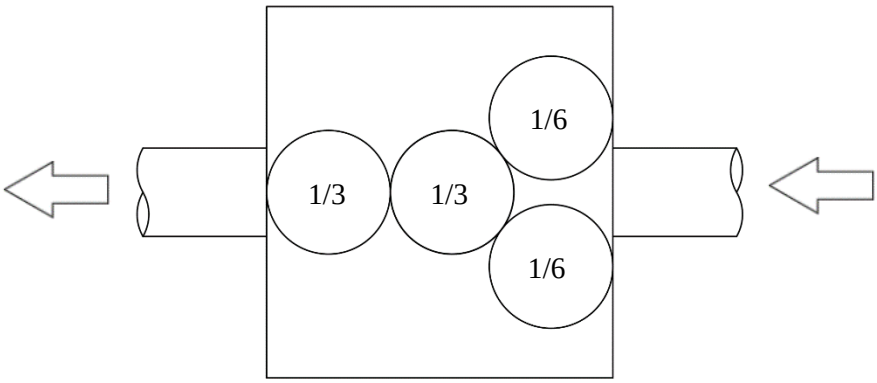

Figure 3-11*: Layout of petri dishes in sump tank with initial sediment proportions*

- By distributing the influent sediment masses in this way, the sump efficiency could be measured in relation to three defined zones, namely the inlet zone, central zone, and outlet zone.
- The required baffle configuration was constructed. Control tests with no baffles placed in the sump were also carried out for comparative purposes.
- The pump inlet valve was opened, and the pumps were turned on.
- Once the water levels of all tanks had stabilised (indicating that a steady-state flow had been achieved), a timer was set for a period of twenty minutes.
- Once the allocated twenty minutes had lapsed, the pumps were turned off, and the pump inlet valve closed.
- Once all flow had ceased and any resuspended sediment in the sump had settled, the drainage valve of the sump tank was opened and allowed to drain completely.
- The Petri dishes were removed from the sump, and the sediment samples were transferred to a beaker.
- The suction pump setup was constructed by connecting the Erlenmeyer flask to the pump, fitting the porous stone on top of the flask, placing the filter paper (previously weighed) on the porous stone, and placing the glass funnel over the filter paper and clamping the funnel to the porous stone.
- The pump was turned on, and the content of the beaker was transferred to the vacuum pump setup for additional drainage.

- After drainage had been completed, the filter paper and semi-dried sediment were transferred to the watch glass (previously weighed) and placed in the oven to dry overnight.
- After drying had been completed, the watch glass was removed from the oven and weighed.
- The retained sediment mass was determined by calculating the difference between the weighed mass and the masses of the watch glass and filter paper recorded at the beginning of the experiment.

The experiment was repeated using three flowrates, three sediment sizes and three influent sediment masses, amounting to twenty-seven tests per sump configuration.

3.8. ADV Experiments

3.8.1. ADV Setup

A *Nortek Vectrino* Acoustic Doppler Velocimeter (ADV) was utilised in experiments to produce vector flow fields for each sump layout. Flow velocity measurements were captured using the device's dedicated software. The ADV was set to its default sampling rate of 25 Hz for data collection.

In order to accurately position the ADV at the required data points for flow velocity capturing, a mounting bracket was built to fit onto the model sump and manoeuvre the ADV in all three degrees of motion.

3.8.2. Experimental Procedure

- Before conducting tests on each baffle arrangement, the same preliminary procedures conducted for the mass-balance tests were followed.
- The required baffle configuration was constructed in the sump tank. In the control test case, no baffles were added to the sump tank.
- The ADV was mounted onto the bracket and positioned at the first data point.
- The ADV was then connected to its power outlet and a computer for data collection.
- All tests were conducted with the flowrate control valve set to the highest measured flowrate from the mass-balance tests to display the most significant variance between high-velocity and low-velocity zones within each baffle arrangement in the model sump.
- The pump inlet valve was opened, and the pumps were turned on.

- Once the water levels of all tanks had stabilised, indicating that uniform flow had been achieved, the data capturing was initiated for a period of thirty seconds, which was chosen as an appropriate measurement of time to account for all variations of flow.

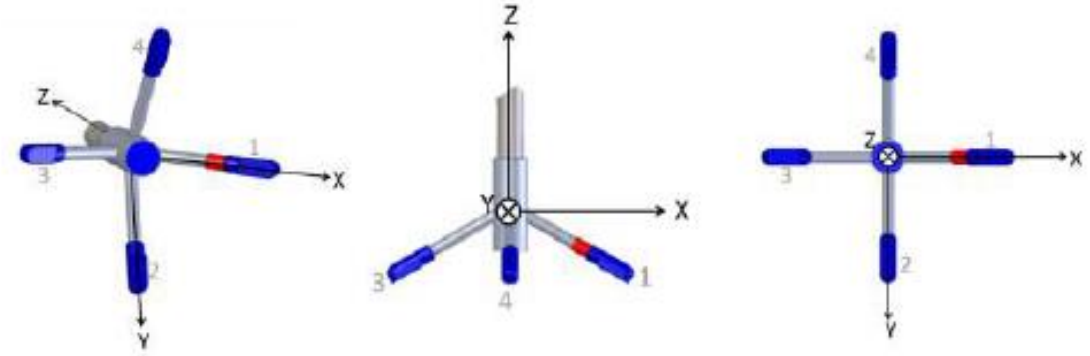

***Figure 3-12**: System of coordinate axes used by the ADV (Nortek, 2021)*

- According to **Figure 3-12**, the flow velocities were measured separately in three degrees of motion (i.e. x, y and z).

- All readings were taken with the positive y-axis facing the sump outlet (the primary direction of flow).
- After the capturing period had ended for the first data point, the ADV mount was manoeuvred to align the ADV with the following data point and data capturing recommenced. This sequence was repeated until all data points chosen for the particular baffle arrangement were completed.
- All readings were taken using the coordinate system shown in **Figure 3-13**. Note that each data plot area was specific to each baffle arrangement, the reason being that many data points could not be measured due to the baffle plates obstructing the ADV and its mounting bracket.

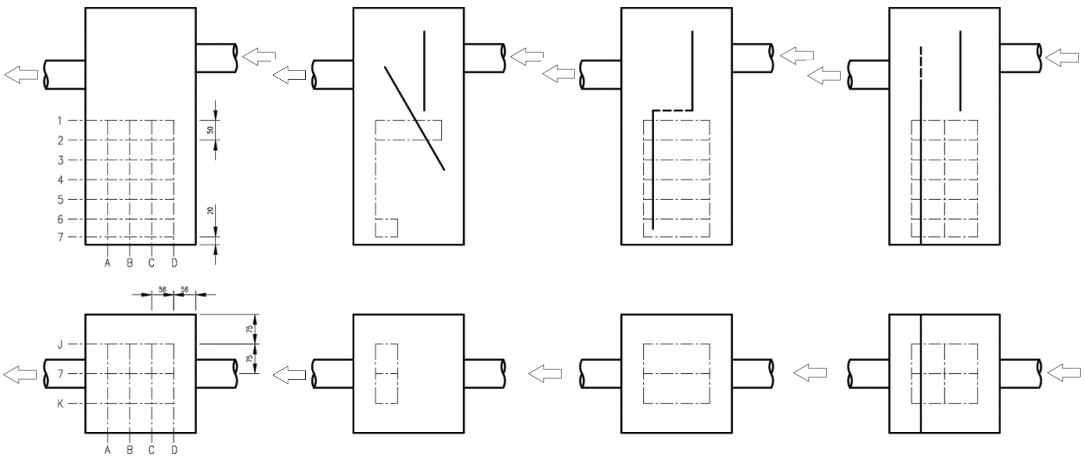

***Figure 3-13**: Coordinate system used by ADV on each baffle arrangement*

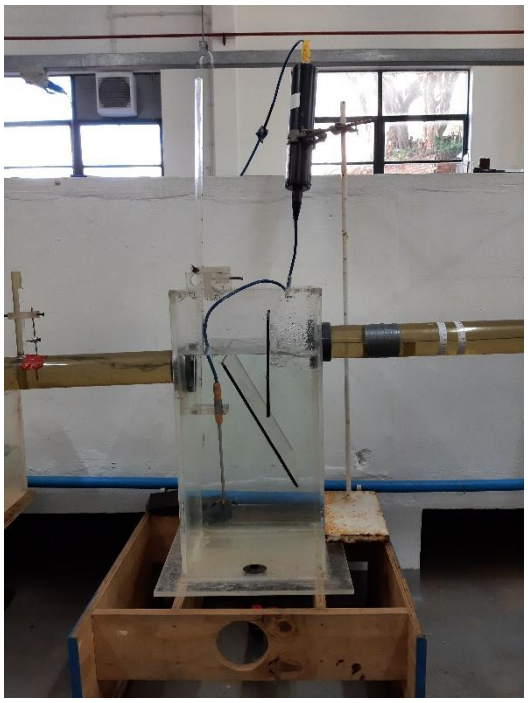

***Figure 3-14**: ADV capturing data for Baffle Arrangement 1*

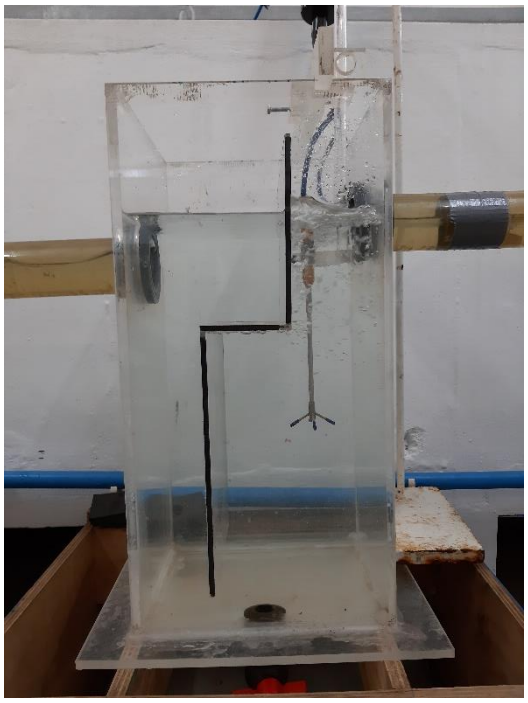

***Figure 3-15**: ADV capturing data for Baffle Arrangement 2*

3.9. Scaling Analysis

3.9.1. Calculation of Dimensionless Parameters

As previously stated in 2.11.2, the results of the mass-balance tests will be converted to non-dimensional variables using the relationship stated in **Equation 2-2**, which relates the sediment washout concentrations to the Péclet and Froude numbers.

3.9.2. Calculation of "True" Parameters

With reference to **Figures 2–1** and **2–2**, an accurate estimation of a typical square-based stormwater sump tank's dimensions would be a 1 m^2 sump bed with a depth of 1,5 m to the stormwater pipeline. These dimensions were used when comparing the model sump to a real stormwater sump

The "*Guidelines and Policy for the Design of Stormwater Drainage and Stormwater Management Systems*" by the Ethekwini Municipality (2008) details methods for determining the magnitude of peak stormwater runoff for urban and rural areas. In these guidelines, the "Rational Method" is performed.

The equation used in the Rational Method is expressed as **Equation 3-3** (Ethekwini Municipality, 2008):

$$Q = ft \times C \times I \times \frac{A}{360} \qquad \textit{(Equation 3-3)}$$

In this equation, ***Q*** (m^3/s) represents the maximum/peak rate of run-off, ***ft*** represents an adjustment factor for the recurrence interval storm considered**,** ***C*** represents the run-off coefficient**,** ***I*** (mm/hr) represents the rainfall intensity, and ***A*** represents the area of the catchment in hectares (1 ha = 10 000m^2)

Notes on how to determine all necessary components of the equation are also provided (Ethekwini Municipality, 2008).

3.10. Sediment Transport Analysis

As stated in **2.10**, the mass-balance test results will also be analysed using Hjulström's Curve (**Figure 2-4**) to measure the level of sediment transport for each sump configuration in relation to the threshold points displayed in this curve.

4. RESULTS AND DISCUSSION

4.1. Introduction

The following chapter provides a discussion and analysis of the results obtained following the experimental tests conducted. In order to accurately and fairly determine the sediment retention efficiencies of all sump configurations, multiple flow rates, sediment grain sizes and influent sediment masses were used for compiling the results of each configuration. As outlined in sections **4.2** and **4.3**, Baffle Arrangement 3 (B3) proved to be the most effective sump configuration tested by the Mass-Balance experiments and ADV experiments.

4.2. Results of Mass Balance Experiments

4.2.1. Flowrates

Three flowrates were used in this experiment to ensure fair analysis results. The flowrates determined using the methods of Samani (2017) are provided in **Table 4-1**:

***Table 4-1**: Calculated experimental flowrates*

Flow Intensity	Flowrate (Q) (l/s)
Low flowrate	0.146
Medium flowrate	0.737
High flowrate	1.315

Calculations of these flowrates are provided in **Table A-1** of **APPENDIX A:**.

4.2.2. Control setup

While conducting tests on the standard sump, the following observations could be made:

The flow pattern within the sump tank followed a distinct elliptical pattern, with the water decelerating upon leaving the sump inlet pipe (due to the sudden increase in elevation head), leading to an almost vertical downward movement when reaching the sump's outlet wall. Around the lower corner of the outlet wall, the constant downward movement of water forces the flow to move almost horizontally across the sump bed. The majority of the scouring and sediment suspension took place in this area. Around the bottom corner of the inlet wall, the force of the

inflowing stormwater discharge from the supply tank forces the flow back up towards the water surface, thus returning to the start of the cycle.

Under higher flowrate conditions, the sediment retention ability of the standard sump decreases exponentially due to a greater volume of water scouring the sump bed, in addition to the suspended sediment being transported out of the sump at a faster rate, thus decreasing the time allowed for resettling to occur.

During the high flowrate tests (where the most defined scouring patterns were achieved), the average dispersion of the remaining sediment in the sump after testing was distributed as shown in **Table 4-2**:

***Table 4-2**: Distribution of retained sediment for Control setup*

Collection Zone	% of Retained Sediment
Inlet Zone	27.34%
Central Zone	26.97%
Outlet Zone	0.44%
Redeposited Sediment	45.25%

The table shows that the smallest proportion of retained sediment was observed in the outlet portion of the sump bed, which aligns with the observations made relating to the presence of high flow velocities in this region. **Table 4-2** also shows that the most significant proportion of sediment retained in the standard sump accounts for sediment that became suspended in the sump and resettled after the stormwater flow ceased. This result is highly unfavourable, as an ideal design should ensure that sediment resuspension is either restricted to the maximum extent or prevented entirely.

With regard to influent sediment masses, an interesting observation was made among the different sediment types. This observation showed that the optimal influent sediment mass for coarse sediment samples was the lowest tested (50 g) under every tested flowrate, and the retention efficiency of the standard sump decreased with the increase of influent sediment mass. However, the optimal sediment mass for the medium and fine sediment samples was the intermediate mass (100 g) for all tested flowrates. This proves that in the case of a standard sump without any baffle arrangement in areas with typically finer influent sediment runoff, an optimal cleaning period could be calculated for the maintenance of the standard sump based on the sediment rate of deposition.

The sediment retention efficiencies (η) calculated after conducting all tests on the control setup are shown in **Figure 4-1**:

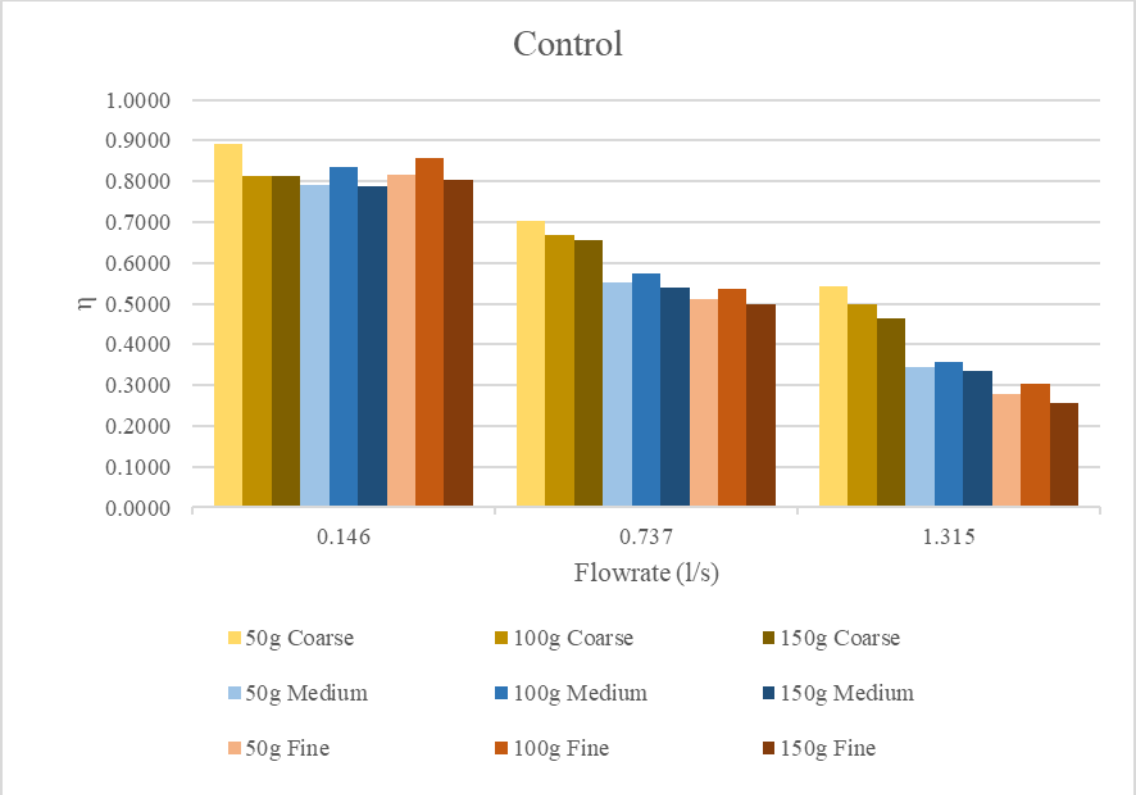

***Figure 4-1**: Sediment retention efficiencies for Control setup*

4.2.3. Baffle Arrangement 1 (B1)

The results of the tests conducted on Baffle Combination 1 surpassed those of the Control setup by improving sediment retention by up to approximately 15%. In the case of the low and medium flowrate tests, all the tests conducted at the same flowrate produced similar sediment retention efficiencies, implying that flowrate was the most significant influence on the efficiency of the baffle arrangement. However, under the high flowrate condition, the sediment retention efficiencies decreased drastically with the increase of influent sediment mass and the decrease of sediment grain size, implying that sediment characteristics are a more significant influence under higher flowrates.

In contrast to the flow pattern produced by the Control setup, the majority of the scouring takes place on the inlet-end of the sump tank due to the 200 mm solid baffle forcing the flow from the inlet pipe vertically downwards toward the inlet-end of the sump bed.

Due to the bottleneck formed underneath the oblique baffle, allowing increased sediment resettling, some sediment transporting took place above the oblique baffle. However, due to the

increase in elevation head as the effluent water travelled over the baffle, a portion of the suspended sediment resettled on the top of the oblique baffle.

The sediment retention efficiencies (η) calculated after conducting all tests on Baffle Arrangement 1 are displayed in **Figure 4-2**:

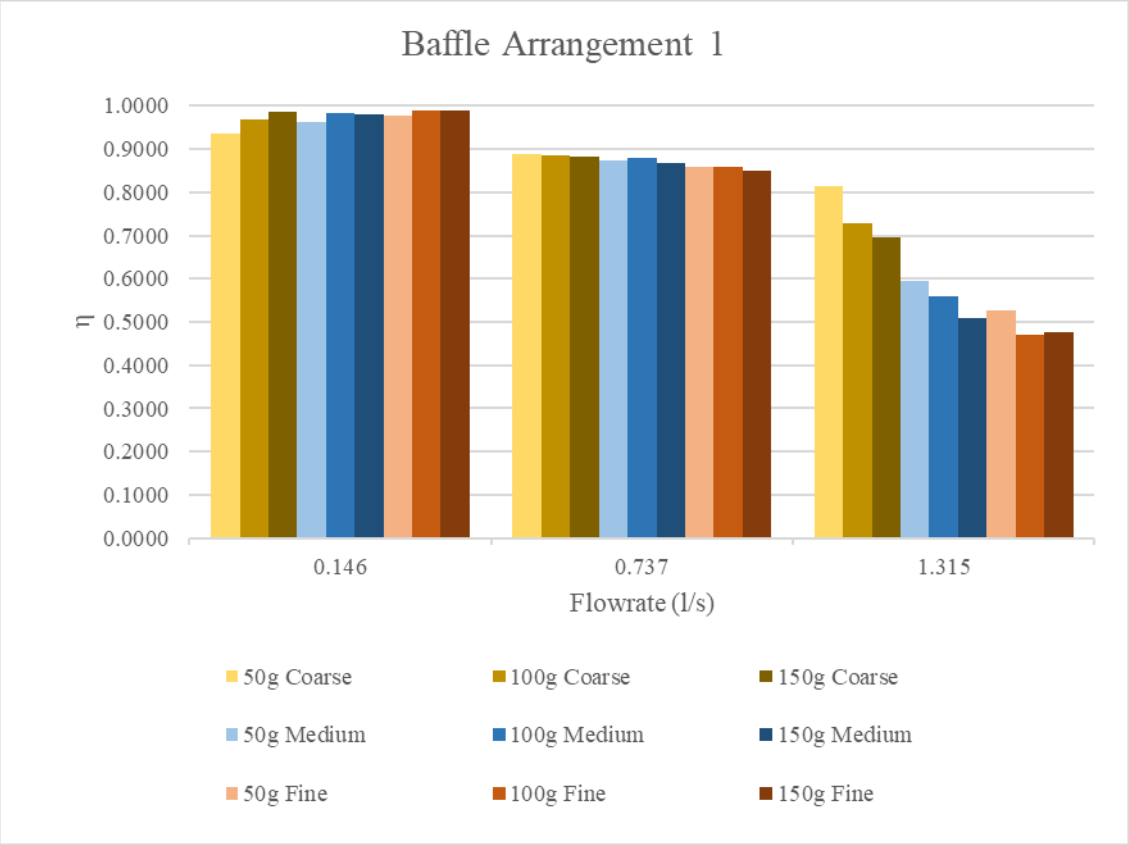

***Figure 4-2**: Sediment retention efficiencies for B1*

A positive outcome worth noting from this data is that the sediment efficiency results for all the tests conducted under low and medium flowrate conditions have little variation (less than 10%), which is highly favourable as it proves that the baffle arrangement's effectiveness is independent of the sediment grain size. However, under the high flowrate condition, this trend does not continue and decreases in a logarithmic fashion with the increase of influent sediment mass and the decrease of sediment grain size, as seen in **Figure 4-2**.

During the high flowrate tests, the average dispersion of the remaining sediment in the sump after testing was distributed as shown in **Table 4-3**:

***Table 4-3**: Distribution of retained sediment for B1*

Collection Zone	% of Retained Sediment
Inlet Zone	0.58%
Central Zone	28.23%
Outlet Zone	56.19%
Redeposited Sediment	15.00%

In **Table 4-3**, the region with the minor proportion of retained sediment has changed compared to the Control setup, from the outlet zone to the inlet zone, due to the change in the flow pattern previously discussed. Another significant observation that can be drawn from **Table 4-3** was that the proportion of sediment redeposited outside the specified collection zones had effectively reduced by a third, which is a highly favourable outcome.

A different trend was observed in terms of influent sediment masses compared to the control setup. Under low flowrate conditions, an increase in influent sediment mass produced higher sediment retention results. However, under the medium and high flowrate conditions, the opposite trend resulted, with the efficiency of sediment retention decreasing when influent sediment mass increased. Through this phenomenon, it is understood that for this baffle arrangement, sediment retention efficiency has a much greater dependency on the magnitude of flow than influent sediment mass in comparison to the control setup. This phenomenon also implies the presence of an optimal flow rate condition for maximum sediment retention efficiency. This optimal flowrate condition can potentially be achieved under practical conditions by designing the portion of the stormwater drainage system upstream of the standard sump to induce this magnitude of flow under peak conditions.

4.2.4. Baffle Arrangement 2 (B2)

The flow paths produced by this baffle arrangement are similar to that of B1 due to scouring occurring closer to the sump inlet than the outlet. For B2, most of the scouring occurred near the centre of the sump bed, but under high flowrates, it acted on the inlet edge due to the flow of water producing a “ricochet” effect off the 200 mm vertical baffle and straight into the bottom corner of the inlet wall. Another major point of scouring is directly under the 300 mm vertical baffle, where water is forced under the small gap in order to pass to the sump outlet.

As previously stated in **3.4.2**, this baffle arrangement provides two possible flow paths for stormwater to follow. The first path is under the 300 mm vertical baffle, which has already been

stated as a point of scouring with minimal resettling due to its proximity to the sump outlet. The second flow path is through the semi-porous baffle, which produces adequate energy losses for resettling.

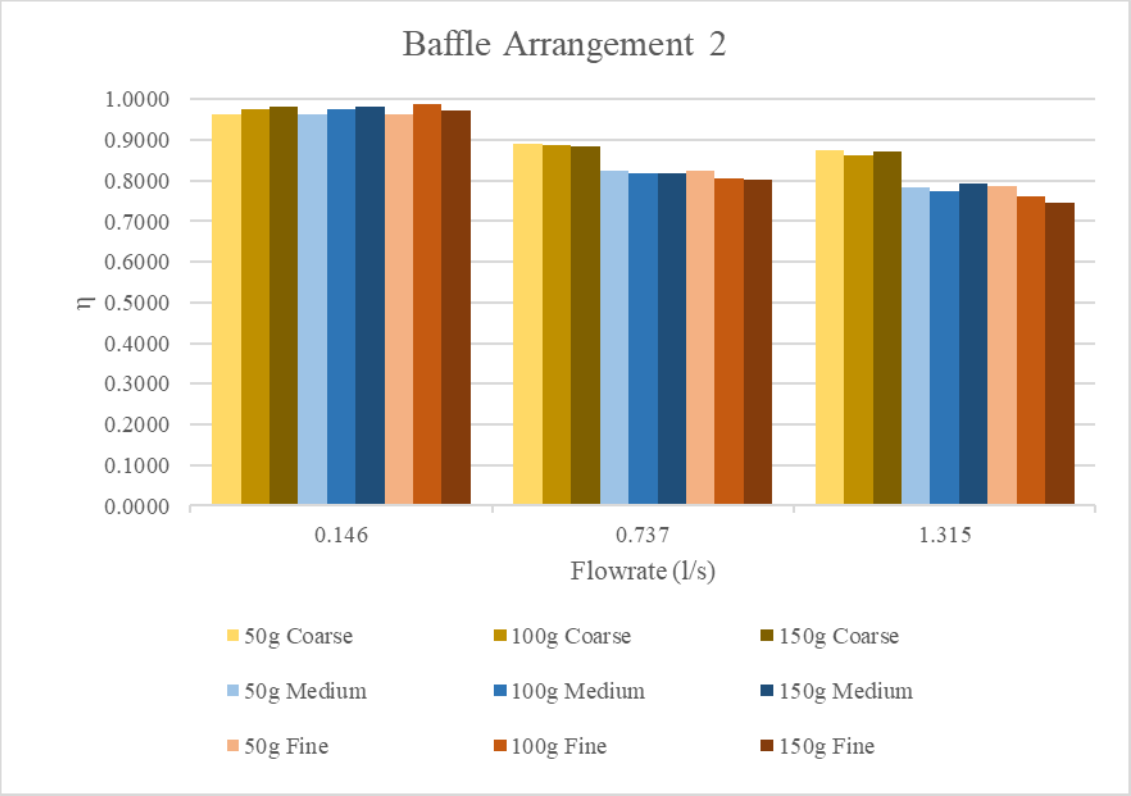

***Figure 4-3**: Sediment retention efficiencies for B2*

The sediment retention efficiencies (η) calculated after conducting all tests on Baffle Arrangement 2 are shown in **Figure 4-3**:

Concerning the low flowrate tests conducted, the same observation in **Figure 4-2** can be seen in **Figure 4-3**. The sediment retention efficiencies calculated have minimal variation, implying that these efficiencies may be independent of sediment grain sizes and influent sediment mass. A similar trend can be seen in the medium and high flow rate tests, but only with regard to the medium and fine sediment samples, as the coarse sediment retention efficiencies under those flow rates exceed the other sediment types by approximately 10% on average.

Further noteworthy observation inferred from **Figure 4-3** shows that the efficiencies calculated for the medium and high flow rate conditions are almost identical. This observation is a highly favourable outcome as it implies that after a certain threshold flowrate is exceeded, the efficiencies produced by this baffle arrangement will decrease minimally or even become independent of the magnitude of flow

During the high flowrate tests, the average dispersion of the remaining sediment in the sump after testing was distributed as shown in **Table 4-4**:

***Table 4-4**: Distribution of retained sediment for B2*

Collection Zone	% of Retained Sediment
Inlet Zone	23.48%
Central Zone	29.65%
Outlet Zone	30.03%
Redeposited Sediment	11.77%

In **Table 4-4**, B2 was able to exceed the improvements made by B1 in respect of two issues. Firstly, the inlet zone retained the smallest proportion of sediment amongst the sump bed, which is much larger than that of B1, thus proving that the extent of scouring at the sump bed has been significantly reduced by using B2. Furthermore, the proportion of sediment suspended and redeposited onto the sump bed had further reduced, implying that B2 had also exceeded the efficiency of B1 in preventing excessive sediment re-entrainment out of the standard sump.

4.2.5. Baffle Arrangement 3 (B3)

This arrangement recorded the best performance of all the baffle arrangements tested. The flow path produced by this baffle arrangement indicates some similarity to that of B2, as the flow of stormwater travels under the 200 mm solid baffle and is forced to flow through the 100 mm semi-porous baffle to reach the sump outlet. However, in contrast to B2, the flow path that travels underneath the 300 mm solid baffle is not present, as the 300 mm baffle had been replaced by the 400 mm solid baffle that joins directly to the sump bed. This change in design effectively removed one of the significant scouring regions present in B2 and largely contributed to this baffle arrangement's highly effective results.

The restriction of flow to a single flow path also played a significant role in the effectiveness of this baffle arrangement. The complementary actions of the 200 mm solid baffle and the (400 mm solid baffle + 100 mm semi-porous baffle) combination forced the stormwater flow into an "S" formation that concentrates the flow to the upper half of the standard sump. Since the stormwater flow is forced to pass through the semi-porous baffle in order to reach the sump outlet, minimal flow is directed towards the lower half of the standard sump, leading to drastically less turbulence in this region and, therefore, minimal sediment re-entrainment. However, the consequence of this design is that the 400 mm solid baffle experiences increased inertial forces from the stormwater

flow being forced upwards into the semi-porous baffle. Under high flow rate conditions, this increased force may cause the solid baffle to shift or possibly cause structural failures such as erosion or cracking. For this reason, the solid baffle should be adequately supported to prevent such failures from occurring in a realistic environment.

Another reason for this arrangement's success over B2 is the change in orientation of the 100 mm semi-porous baffle from a horizontal to a vertical position. This change allowed the semi-porous baffle to interact with the stormwater flow at an increased elevation, reducing the flow velocity. With the semi-porous baffle restricting the movement of a lower flowrate, its effectiveness in assisting any suspended sediment particles with resettling was increased.

The sediment retention efficiencies (η) calculated after conducting all tests on Baffle Arrangement 3 are displayed in **Figure 4-4**:

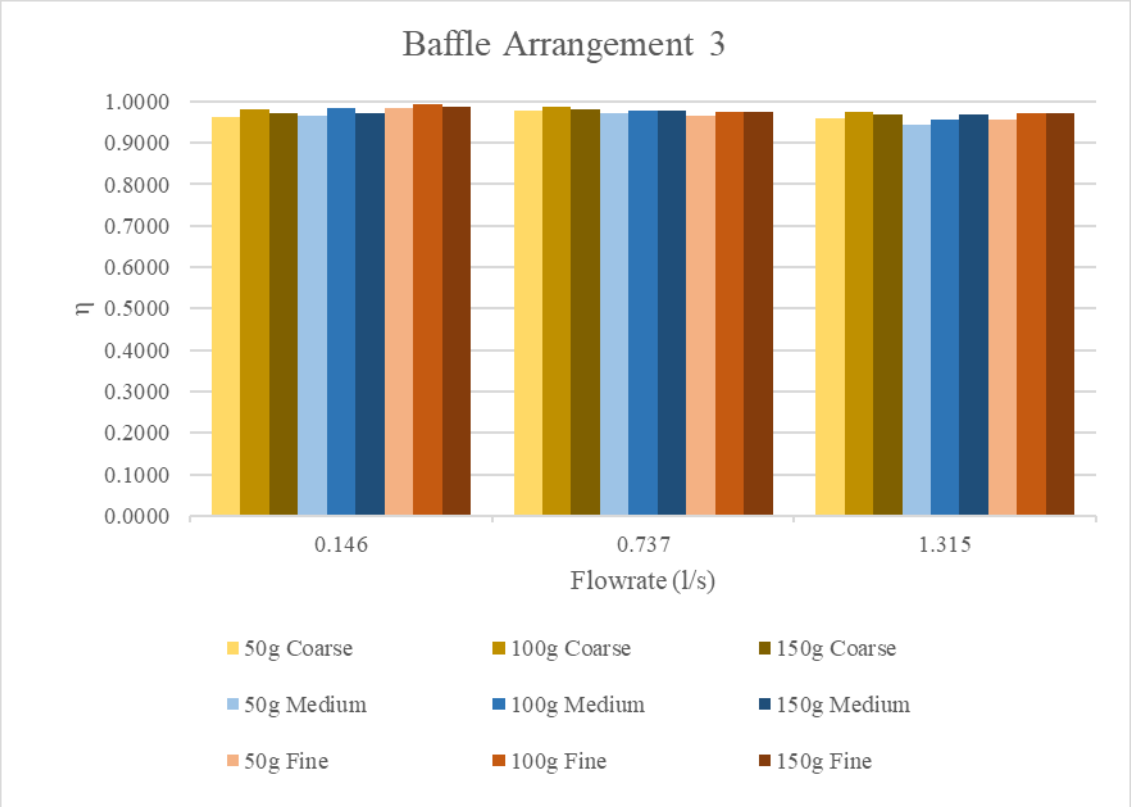

***Figure 4-4**: Sediment retention efficiencies for B3*

As seen in **Figure 4-4**, all efficiencies calculated and recorded range approximately between 94 – 99% sediment retention, the smallest variation in results amongst all the sump configurations. This observation implies that the use of B3 will produce sediment retention efficiencies that are practically independent of sediment grain sizes, influent sediment mass or the magnitude of flow, which is an ideal scenario.

During the high flowrate tests, the average dispersion of the remaining sediment in the sump after testing was distributed as shown in **Table 4-5**:

***Table 4-5**: Distribution of retained sediment for B3*

Collection Zone	% of Retained Sediment
Inlet Zone	33.16%
Central Zone	29.55%
Outlet Zone	35.26%
Redeposited Sediment	2.03%

In **Table 4-5**, B3 produced the least sediment redistribution of all the sump configurations. The region that experienced the most sediment re-entrainment was the central zone. However, the level of scouring was minute compared to the other sump configurations. Another insight presented in **Table 4-5** shows that the proportion of sediment redistributed outside the collection zone was also extremely minute compared to the other sump configurations. These observations indicate that this baffle arrangement is capable of producing near-ideal sediment retention results.

The calculations related to all washout efficiencies can be found in **Table B-1 to B-4** of **APPENDIX B:**.

4.3. Results of ADV Experiments

4.3.1. Control setup

Figure 4-5 below shows that the vertical velocity profile validates the claim made in section **4.2.2** regarding the "elliptical" flow pattern observed when using a standard sump without any baffle arrangements. The figure shows a significant range of flow velocities within the standard sump.

As previously mentioned, the flow velocity is at its lowest at the top of the sump tank, specifically towards the outlet end of the sump. In contrast, the flow velocity is highest at the sump bed. In the case of the horizontal velocity profile, it was observed that the high flow velocity region is within the outlet end and central regions of the sump. At the outlet end specifically, the most significant downward vertical component of velocity was observed; therefore, this region would produce the most significant proportion of scouring on the sump bed. Compared to the scouring pattern observed in **Figure 4-6**, this is indeed the case.

In the horizontal velocity profile, a slight asymmetry can be observed in the directionality of the flow. This observation can be explained by the presence of the sump tank drainage valve producing a ripple in the flow against the sump bed. This occurrence can also be seen in the scour pattern below.

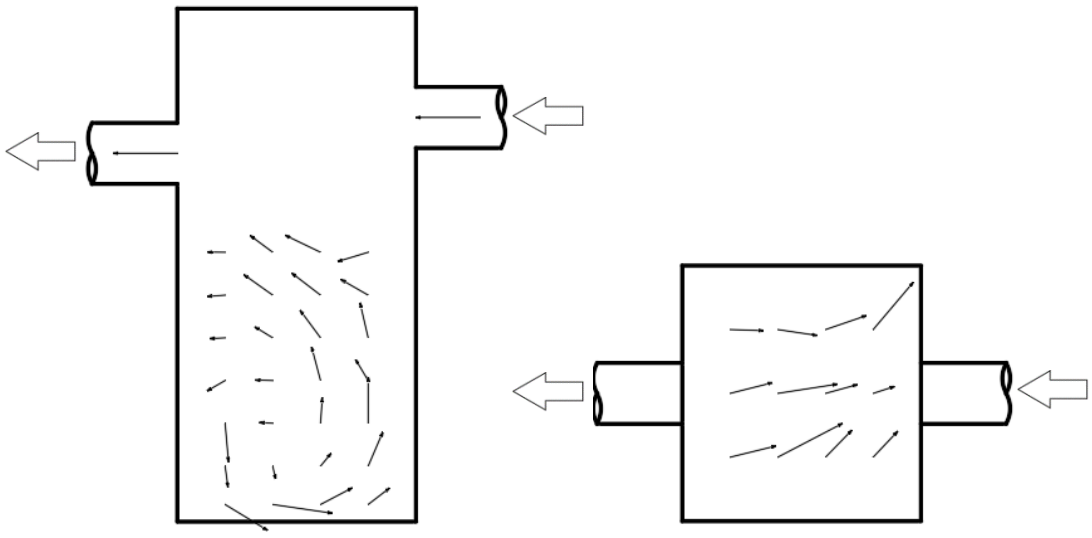

***Figure 4-5**: Flow velocity profiles of Control setup*

***Figure 4-6**: Scouring pattern of Control setup*

4.3.2. Baffle Arrangement 1 (B1)

The presence of the oblique baffle practically spanning across the entire sump tank in the baffle arrangement attributed to difficulties in the data collection processes. For this reason, the velocity profiles produced are the smallest of all the arrangements tested.

Three distinct regions can be observed in the vertical profile displayed in **Figure 4-7**. The two data points measured below the sump inlet depict a high-velocity flow split along two paths, one between the vertical and oblique baffles and the other under the oblique baffle.

The second region is the high-velocity zone measured towards the outlet end of the sump tank at the base of the sump. Although the other data points near the sump bed could not be measured, a strong assumption can be made that this area also forms part of this high-velocity zone due to the sudden drop in elevation paired with the increased pressure required to pass through the gap created by the oblique baffle causing a significant increase in velocity at the base of the sump near the inlet end. This region would also have the greatest vertically downward velocity component, causing most of the scouring to occur there. This claim is confirmed by the scouring pattern produced in **Figure 4-8**.

The final region of note is the low-velocity zone observed on the outlet end of the sump tank, located directly below the outlet pipe. The flow velocities measured at the central depth of this region were extremely low, thus implying the existence of a “dead zone” in this area where it is more than likely where the majority of the sediment resettling took place. This claim is validated by the scour pattern below.

Regarding the horizontal profile, the most significant observation was that, although the baffle arrangement was able to switch the flow direction at the sump bed, the magnitude of the flow velocity remained unchanged. Therefore, this observation implies that the amount of sediment scouring occurring in the sump remains the same. In conclusion, the evidence proves that this baffle arrangement would not be exceedingly effective for sediment retention.

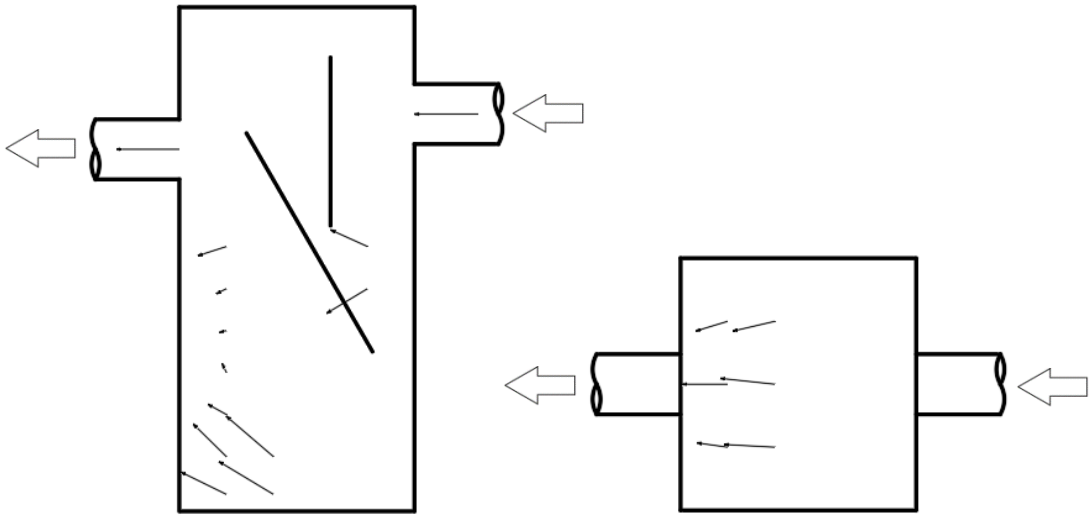

***Figure 4-7**: Flow velocity profiles of Baffle Arrangement 1*

***Figure 4-8**: Scouring pattern of Baffle Arrangement 1*

4.3.3. Baffle Arrangement 2 (B2)

Similarly to B1, this arrangement also proved difficult to extract and capture data from due to the restricted access to the centre of the sump tank created by the horizontal semi-porous baffle.

In the vertical profile captured in **Figure 4-9**, the flow pattern can be divided into six distinct regions. Below the sump inlet, the first region is observed where the flow path splits in two directions at high velocities: one path directed towards the semi-porous baffle and the other directed towards the opening between the sump bed and the 300 mm solid baffle.

The second region is shown just below the first, where a low-velocity eddy can be seen circulating the stormwater at the mid-depth of the sump. This region is favourable to the resettling of suspended sediment, as the sediment is circulated away from the sump outlet and allowed to settle due to the low flow magnitude.

The third region can be seen below the eddy, where the stormwater flow begins to direct itself horizontally, parallel to the sump bed and towards the opening under the 300 mm solid baffle. Sediment scouring did take place in this region of the sump bed but was not excessive, as the magnitude of the flow velocity was relatively small.

The fourth region is the high flow velocity area between the 300 mm solid baffle and the sump bed. This region has such high flow velocities due to the sudden reduction in cross-sectional area for the stormwater to pass through. Subsequently, this region received the most significant sediment scouring, which is visible in **Figure 4-10**.

The fifth region is shown on the side of the 300 mm baffle facing the sump outlet, where low-velocity flows can be seen travelling downwards towards the sump bed. This region may be influenced by the sediment that had lost energy while moving upwards through the horizontal semi-porous baffle and was now settling due to those energy losses rather than being transported up to the sump outlet. Therefore, this region was ideal for inducing the re-settling of sediment that had become suspended.

The sixth and final region can be seen below the sump outlet, starting from the horizontal semi-porous baffle. In this region, sediment is carried upward and through the sump outlet. While the directionality of flow in this region is away from the sump bed, the magnitude of flow seems relatively small and may allow for resettling to occur.

Regarding the horizontal flow velocity profile, it is observed that most of the flow velocities around the sump bed have favourably decreased compared to the previous sump configurations, leading to reduced scouring of the sump bed. However, the flow velocity located in the central outlet region of the sump bed is much larger than any other vectors measured in previous sump configurations, the reason being that this area forms the fourth region of the vertical profile previously discussed.

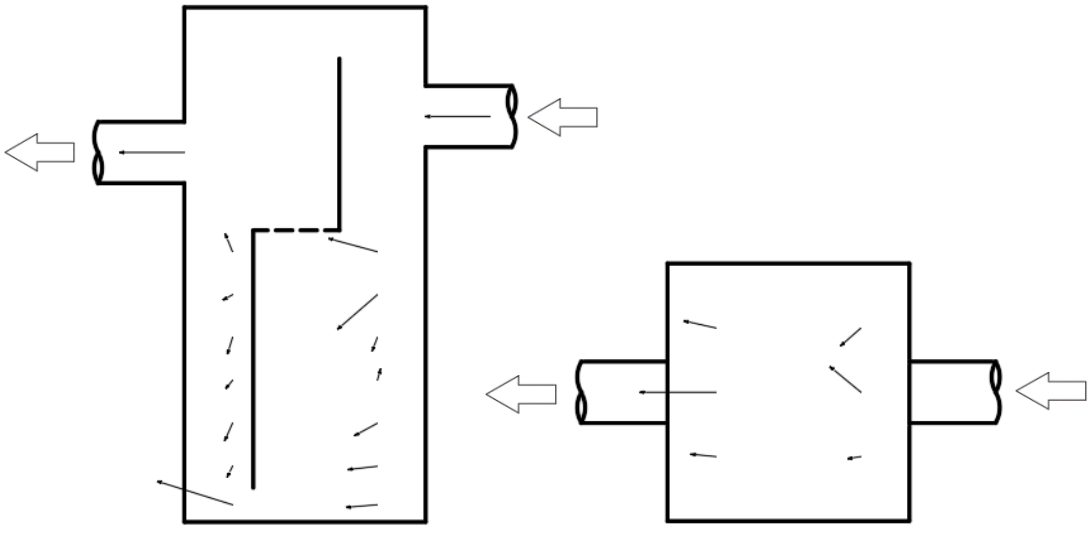

***Figure 4-9**: Flow velocity profiles of Baffle Arrangement 2*

***Figure 4-10**: Scouring pattern of Baffle Arrangement 2*

4.3.4. Baffle Arrangement 3 (B3)

This baffle arrangement produced velocity profiles unlike any of the previous sump configurations. Furthermore, the velocity profiles measured in this profile include the smallest flow velocities recorded from all the sump configurations tested. Both observations form the reasoning as to why this baffle arrangement performed as exceptionally as it did amongst all the sump configurations tested.

With respect to the vertical flow velocity field (shown in **Figure 4-11**), three unique flow interactions could be observed in the inlet, central and outlet regions of the model sump. A similar interaction to Baffle Arrangements 1 and 2 is seen in the inlet region, where the stormwater flow moves under the 200 mm solid baffle at a high velocity. However, unlike the other baffle arrangements, the vertical velocity component is not upwards toward the sump outlet but somewhat horizontally towards the 400 mm solid baffle. At mid-depth, the magnitude of flow velocity in this direction was at its highest and gradually decreased with the increase of depth until the magnitude had reached a constant value within the last 100 mm of the sump bed.

At the central region, the directionality of flow for all the measured data points in that area follows a course towards the 400 mm solid baffle at mid-depth, increasing in magnitude as the flow moves closer to this point. The most significant magnitude of flow within this baffle arrangement is

positioned at this mid-depth area of the central region and travels perpendicularly towards the 400 mm solid baffle (similarly to the flow pattern observed at the inlet region).

This phenomenon is attributed to the strong inflow current concentrating the flow towards this point. These observations validate the statement made in **4.2.5** regarding the need for adequate support of the solid baffle under practical conditions.

At the outlet region, three flow interactions can be observed. The first is observed below mid-depth, where a hydraulic "dead zone" can be seen where the measured flow is practically non-existent. Secondly, at mid-depth, the flow can be seen moving at a relatively low velocity in a horizontal direction towards the 400 mm solid baffle. This interaction is due to the stormwater flow resisting the forces being applied on the other side of the 400 mm solid baffle. Finally, above mid-depth, the stormwater flow can be seen changing direction, moving towards the sump outlet at low velocity. In general, this region is ideal for resettling suspended sediment particles due to the low-velocity flows and hydraulic "dead zone" observed.

Regarding the horizontal flow velocity profile, this baffle arrangement produced the lowest flow velocities recorded of all the sump configurations tested, thus validating the reason for it being the best-performing configuration. The reasoning behind its success was due to the baffle arrangement concentrating the stormwater flow towards the mid-depth of the sump tank rather than the sump bed, as previously discussed. In this profile, the area with the highest flow velocity was the inlet region; therefore, most of the scouring experienced at the sump bed would be in this region. This observation is validated by the scouring pattern shown in **Figure 4-12**.

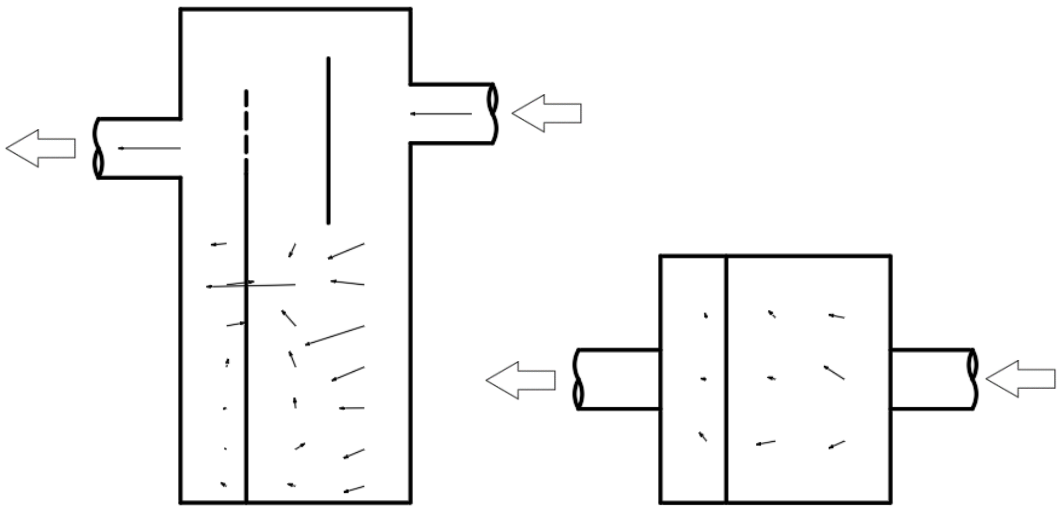

***Figure 4-11**: Flow velocity profiles of Baffle Arrangement 3*

***Figure 4-12**: Scouring pattern of Baffle Arrangement 3*

4.3.5. Observations made during ADV operation

As previously mentioned, the measurement of flow velocities throughout the standard sump proved difficult for the ADV within specific baffle arrangements. While this may be seen as an unfavourable outcome for the capturing of data, it can also be seen as an insight into the convenience of maintenance for each baffle arrangement. The same areas within the standard sump model where the ADV could not capture data would also be areas in a practical setting where cleaning and maintenance equipment would not be able to reach. With this understanding, B1 would be the most challenging baffle arrangement to perform routine maintenance, and B3 would be the most convenient for cleaning and other maintenance. As B3 is the most effective baffle arrangement and the most convenient in a practical setting, it would be an ideal design for installation in stormwater standard sumps.

All averaged readings captured by the ADV for each sump configuration can be found in **Table C-1** to **C-4** of **APPENDIX C**:.

4.4. Head losses

Due to the experimental setup having a closed-circuit flow, the velocity head experienced at the inlet and outlet of the sump are identical. Therefore, the difference in head losses between the control setup and the baffle arrangement setups could not be fairly measured, with the only tangible head loss experienced for all tests being the constant difference of 42mm in elevation heads between the sump inlet and outlet pipes. Although this issue prevents the measurement of changes in headloss amongst all sump configurations, the flow fields derived from the ADV show the ability of the baffle arrangements to reduce velocity heads within the model sump in comparison to the control setup.

Furthermore, it is worth mentioning that under high flowrate conditions, where "short-circuiting" or "through-flow" can be achieved, the head loss may have further decreased to a negligible value due to the outflow pipe being insufficient for large volumes of water to pass through.

4.5. Results from Sediment Transport Diagram

All sump configurations were compared using the most unfavourable condition tested for all configurations (high flow rate, fine sediment, and high influent mass). The Hjulström's Curve analysis showed that B3 significantly outperformed the other configurations' ability to prevent sediment re-entrainment by providing the closest condition to the "Sedimentation/Transportation" threshold curve compared to the other configurations. These results further validate B3's performance as the most effective sump configuration tested.

The application of this diagram can be found in **Figures D-1** of **APPENDIX D:.**

4.6. Results of Scaling Analysis

4.6.1. Deriving Washout Functions

From the results of the dimensional analysis based on **Equation 2-2**, the following washout functions were produced:

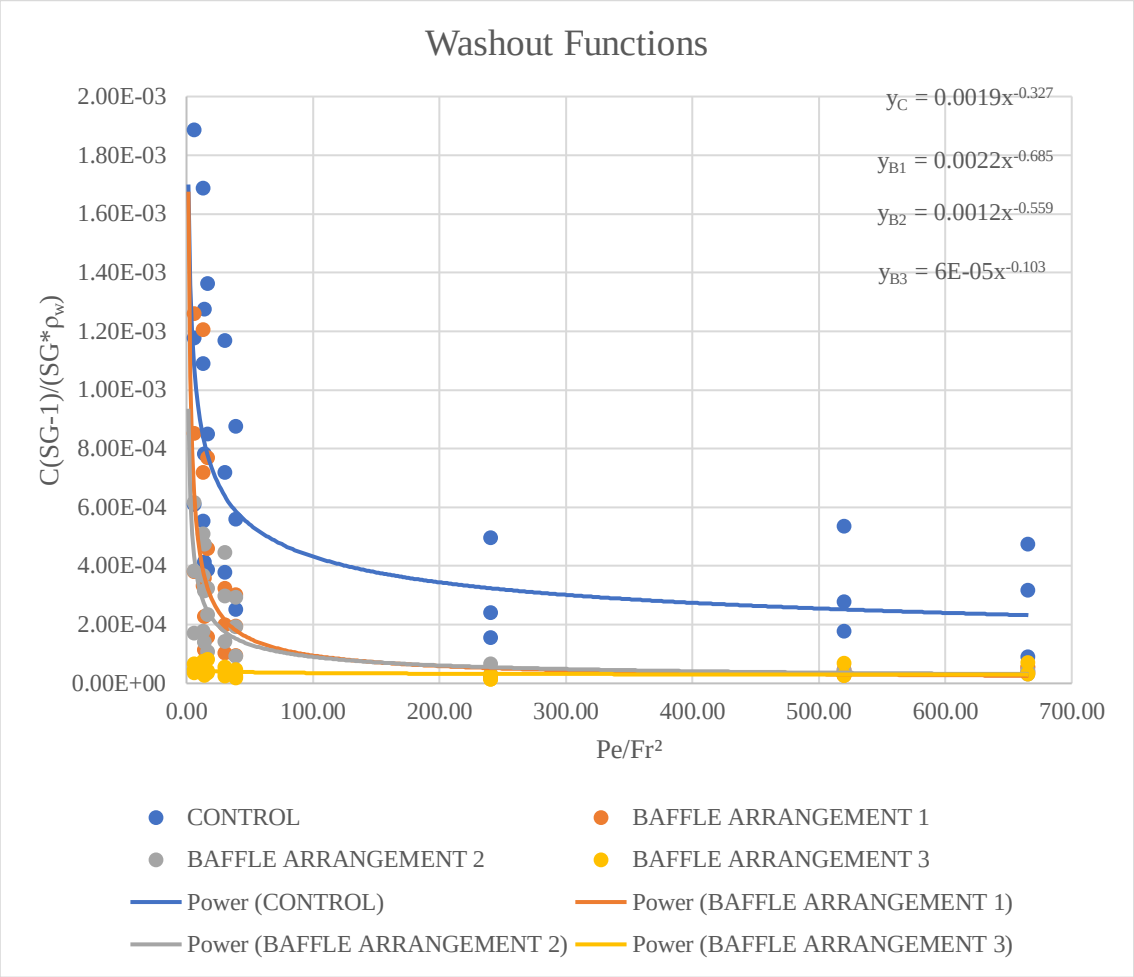

***Figure 4-13**: Washout function of all sump configurations*

As observed by the graph, all baffle arrangements performed exceptionally well to prevent sediment washout compared to the control setup. This observation is depicted by the washout curves of the baffle arrangements forming much lower than that of the control condition.

Of the three design setups, B3 is displayed as having the best design tested since it has the lowest washout curve of all the configurations. With reference to **Equation 2-2**, the washout function may be expressed as follows:

$$\frac{C(SG-1)}{\rho_w SG} = 6 \times 10^{-5} \left(\frac{Pe}{Fr^2}\right)^{-0.103}$$

The calculations for these results can be found in **Table E-1** of **APPENDIX E**:.

When compared to the washout function achieved by the SAFL baffle used by Howard *et al.* (2012), it is apparent that the washout functions of baffle arrangements B1, B2 and B3 are lower than this function (**Figure 4-14**). This is a favourable outcome as it displays that the results of this study have successfully surpassed that of previous research.

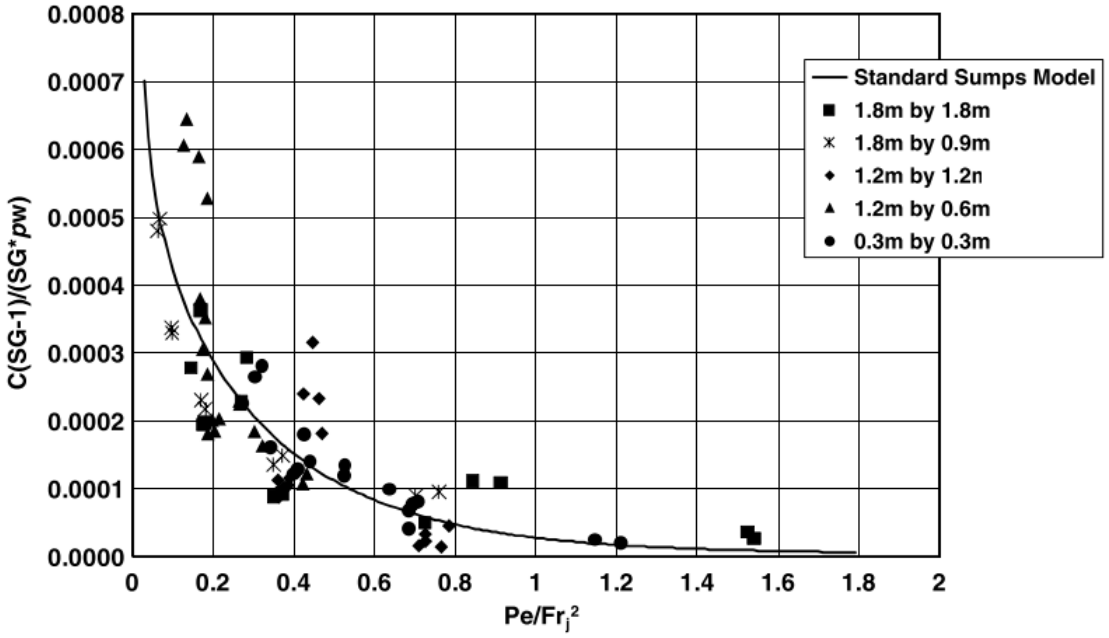

Figure 4-14: *Washout function and experimental data for standard sumps tested (Howard et al., 2012)*

4.6.2. Application of Washout Function

With the use of the derived washout functions, the sediment retention efficiencies produced during experimentation can be replicated in a practical setting. This is achieved by entering the required flow rate and sediment conditions for a sump to be designed, which returns an equation for the optimal dimensions for that sump as an output. For example, if a standard sump is designed to hold sediment particles ranging from 75 – 106 µm with 97.24% efficiency at 1.315 l/s using B3, the value of Pe/Fr^2 would equate to 6.08 (refer to **Table E-1**). The expansion of this equation produces the following:

$$\frac{\frac{U_s h L}{Q}}{\frac{u^2}{gL}} = 6.08$$

Practically, the particle settling velocity and inlet velocity can be determined through annual data on the particle size distribution and rainfall trends collected from the proposed area of installation

and the design of the stormwater drainage system, respectively. Calculation of the equation with these values produces the result $hL^2 = 0.036\ m^3$. From this point, the dimensions of the standard sump can be optimised based on the limiting variable, either limited plan area or limited excavation depth.

Assuming the typical dimensions and peak flowrate of a standard sump discussed in **3.9.2**, applying the washout function for Baffle Combination 3 produces an effluent concentration of approximately 0.4 kg/m^3, which is a highly effective result (granted that cleaning and maintenance are conducted regularly).

4.7. Real-world application

The fact that Baffle Arrangement 3 is the preferred baffle arrangement is beneficial from a practical and operational point of view. As previously discussed, B3 is structurally the simplest of the three designs, which will allow for quick and straightforward installation of the arrangement into new and pre-existing stormwater sumps. The design will also allow easier access to the sump bed for cleaning and maintenance purposes.

While the calculated effectiveness of B3 under real-world conditions is significant, it should be noted that the result of the washout function is an idealised value and may vary from the true effectiveness. This may be attributed to the limitations and assumptions stated in **3.3**, as well as the fact that sediment transport does not strictly follow Froudian law. Although the washout function provides a fair estimate of the baffle arrangement's effectiveness, the testing of a prototype would provide the most definitive results.

5. CONCLUSION

5.1. Overview

Within stormwater drainage systems, the issue of sediment transport is an ongoing challenge, with most research prioritising the trapping of sediment over the prevention of sediment washout. Therefore, this research explored finding the best baffle arrangement that would provide optimal results for minimizing sediment washout.

This study aimed to determine the most effective baffle arrangement that would minimise sediment resuspension and washout in a stormwater standard sump and determine the baffle arrangement's effectiveness in a practical setting.

This was executed by conducting tests on a stormwater sump model to determine the washout efficiencies of different baffle arrangements. Flowrates, sediment sizes and influent sediment masses were varied to produce fair and unbiased results.

From the results of these tests, the best baffle arrangement was determined using simple mass balance techniques. All baffle arrangement configurations outperformed the control setup, with Baffle Arrangement 3 (B3) performing the best overall. B3's sediment retention effectiveness performed consistently, independent of all variable conditions, making it the ideal baffle arrangement tested.

The flow velocity profiles of each sump configuration were then analysed using an ADV to validate these results. The flow fields produced by the baffle arrangements clearly displayed how the baffles worked to reduce turbulent flow within the model sump and minimise the re-entrainment of suspended sediment particles. B3 was observed to produce the most significant low-velocity area at the sump bed compared to the other sump configurations, allowing for optimal sediment retention and further validating the results of the mass-balance experiments.

Finally, a scaling analysis was also conducted to determine the relationship between the results produced by the model sump and the possible effectiveness of a standard sump. A Washout Function was produced from this analysis, allowing the calculation of the potential sediment retention effectiveness of B3 under practical conditions.

5.2. Response to Research Questions

Based on the results of this study, a confident statement can be made that Baffle Combination 3 is an effective design for the optimisation of sediment retention in stormwater standard sumps. Based on the scaling analysis of the results produced, it can also be stated that this design will produce effective retention results under real-life conditions.

5.3. Recommendations for future research

The following recommendations may be made for future testing on sediment transport in stormwater sumps:

During the investigation, only steady flow conditions were considered when testing the efficiencies of the baffle arrangements. In a practical setting, the stormwater flow would be variable and dependent on the changes in rainfall density during a storm event. Therefore, in future research, variable flowrates should be considered.

With the consideration of variable flowrates comes the issue of measuring the rate of sediment washout with the variation of flow. A possible solution to this issue would be the installation of strain gauges to the sump bed, as this would provide instantaneous measurements of the changes in sediment mass within the standard sump.

This method of measuring sediment retention would also prevent discrepancies caused by a loss of sediment during transportation out of the model sump and would also remove the need for petri dishes, allowing for more accurate sediment transport during testing because of the removal of shear resistances.

Using an ADV to measure flow velocity fields within the model sump proved difficult due to the restrictions created by the baffle plates. A solution to this issue would be to consider less invasive measurement techniques, such as Particle Image Velocimetry (PIV).

As stated in **4.7**, experimentation on a scale prototype sump would provide the most definitive results of the baffle arrangements' effectiveness for sediment retention. The prototype could be tested under practical conditions where head losses could be accurately measured. Furthermore, the results of this experiment can be compared to the results derived from the washout function to determine its level of accuracy.

REFERENCES

Alam, M. Z. *et al.* (2018) 'Improving stormwater quality at source using catch basin inserts', *Journal of Environmental Management*, 228, pp. 393–404. doi: 10.1016/J.JENVMAN.2018.08.070.

Armitage, N. (2007) 'The reduction of urban litter in the stormwater drains of South Africa', *Urban Water Journal*, 4(3), pp. 151–172. doi: 10.1080/15730620701464117.

Asgharzadeh, H., Firoozabadi, B. and Afshin, H. (2011) 'Experimental investigation of effects of baffle configurations on the performance of a secondary sedimentation tank', *Scientia Iranica*, 18(4 B), pp. 938–949. doi: 10.1016/j.scient.2011.07.005.

Badge, D. (2019) *Assessment of sediment trapping efficiency in the standard stormwater sump with different baffle arrangements*. University of KwaZulu-Natal.

Basham, D. L., Zech, W. C. and Donald, W. N. (2019) 'Evaluating catch basin inserts (CBI) as a post-construction sediment removal tool for Ohio roadways', in *IECA Annual Conference and Expo 2019*. Available at: https://www.engineeringvillage.com/share/document.url?mid=cpx_M2c01774616ab1fe839bM707d10178163167&database=cpx&view=detailed (Accessed: 16 November 2021).

Chien, N. and Wan, Z. (1999) *Mechanics of Sediment Transport*. Reston, VA: American Society of Civil Engineers. doi: 10.1061/9780784404003.

Davidson, L. (2015) 'Fluid mechanics, turbulent flow and turbulence modeling'. Available at: http://citeseerx.ist.psu.edu/viewdoc/summary?doi=10.1.1.703.5520 (Accessed: 9 February 2022).

Dueñas Díez, M. *et al.* (2002) 'Simulation of a hydrometallurgical leaching reactor modeled as a DAE system', *Modeling, Identification and Control*, 23(2), pp. 93–115. doi: 10.4173/MIC.2002.2.2.

Ethekwini Municipality (2008) 'Engineering Unit Coastal Stormwater & Catchment Management Department Design Manual : Guidelines And Policy For The Design Of Stormwater Drainage And Stormwater Management Systems (Vade Mecum) Ethekwini Municipality Design Manual : Guidelines And Policy', (May), pp. 1–50.

Fan, C. Y. *et al.* (2001) 'Sewer and tank flushing for sediment, corrosion, and pollution control', *Journal of Water Resources Planning and Management*, 127(3), pp. 194–201. doi: 10.1061/(ASCE)0733-9496(2001)127:3(194).

Faram, M. G. and Harwood, R. (2002) *A method for the numerical assessment of sediment interceptors Characterisation of sediments captured by stormwater separators View project A Method for the Numerical Assessment of Sediment Interceptors*. Available at: https://www.researchgate.net/publication/270685488 (Accessed: 21 October 2020).

Farjood, A., Melville, B. W. and Shamseldin, A. Y. (2015) 'Optimisation of baffles for sediment retention ponds'.

Fondriest Environmental, I. (2022) *Sediment Transport and Deposition - Environmental Measurement Systems*. Available at: https://www.fondriest.com/environmental-measurements/parameters/hydrology/sediment-transport-deposition/ (Accessed: 26 May 2022).

Frankel, M. (2012) 'STORMWATER DRAINAGE AND DISPOSAL'. Available at: https://www.accessengineeringlibrary.com/content/book/9780071760270/chapter/chapter17 (Accessed: 7 February 2022).

Glasbergen, K. *et al.* (2014) 'The effect of coarse gravel on cohesive sediment entrapment in an annular flume', *IAHS-AISH Proceedings and Reports*, 367(December 2014), pp. 157–162. doi: 10.5194/piahs-367-157-2015.

Haris, H. *et al.* (2016) 'Urban Stormwater Management Model and Tools for Designing Stormwater Management of Green Infrastructure Practices', *IOP Conference Series: Earth and Environmental Science*, 32(1), p. 012022. doi: 10.1088/1755-1315/32/1/012022.

Howard, A. *et al.* (2011) 'SAFL Baffle retrofit for suspended sediment removal in storm sewer sumps', *Water Research*, 45(18), pp. 5895–5904. doi: 10.1016/j.watres.2011.08.043.

Howard, A. K. *et al.* (2012) 'Hydraulic Analysis of Suspended Sediment Removal from Storm Water in a Standard Sump', *Journal of Hydraulic Engineering*, 138(6), pp. 491–502. doi: 10.1061/(ASCE)HY.1943-7900.0000544.

Howard, A. K., Stefan, H. G. and Mohseni, O. (2010) 'Use of Standard Sumps for Suspended Sediment Removal from Stormwater', *Civil Engineering / Graduate School*, Masters(June), p. 58.

Ma, Y. and Zhu, D. Z. (2014) 'Improving sediment removal in standard stormwater sumps', *Water Science and Technology*, 69(10), pp. 2099–2105. doi: 10.2166/wst.2014.122.

Montakhab, A. *et al.* (2012) 'Flow and sediment transport in vegetated waterways: A review', *Reviews in Environmental Science and Biotechnology*, 11(3), pp. 275–287. doi: 10.1007/S11157-012-9266-Y.

Nighman, D. M. and Harbor, J. M. (1997) 'Trap Efficiency of a Stormwater Basin with and

Without Baffkes', *Proc. Int. Erosion Control Assn 28*, pp. 469–483.

Nortek (2021) *The Comprehensive Manual for Velocimeters*.

Pretorius, C. F. (2012) 'A review of vortex grit basin design', *WEFTEC 2012 - 85th Annual Technical Exhibition and Conference*, 9(January 2012), pp. 5715–5734. doi: 10.2175/193864712811709382.

Quang, C. N. X. *et al.* (2022) 'Effects of sediment deposit on the hydraulic performance of the urban stormwater drainage system', *IOP Conference Series: Earth and Environmental Science*, 964(1), p. 012020. doi: 10.1088/1755-1315/964/1/012020.

Rapp, B. E. (2016) 'Microfluidics: Modeling, mechanics and mathematics', *Microfluidics: Modeling, Mechanics and Mathematics*, pp. 1–766. doi: 10.1016/C2012-0-02230-2.

Sahin, C., Ozturk, M. and Aydogan, B. (2020) 'Acoustic doppler velocimeter backscatter for suspended sediment measurements: Effects of sediment size and attenuation', *Applied Ocean Research*, 94(October 2019), p. 101975. doi: 10.1016/j.apor.2019.101975.

Samani, Z. (2017) 'Three Simple Flumes for Flow Measurement in Open Channels', *Journal of Irrigation and Drainage Engineering*, 143(6), p. 04017010. doi: 10.1061/(asce)ir.1943-4774.0001168.

Selbig, W. R. *et al.* (2016) 'The effect of particle size distribution on the design of urban stormwater control measures', *Water (Switzerland)*, 8(1), p. 17. doi: 10.3390/w8010017.

Shahrokhi, M. *et al.* (2013) 'Experimental investigation of the influence of baffle position on the flow field, sediment concentration, and efficiency of rectangular primary sedimentation tanks', *Journal of Hydraulic Engineering*, 139(1), pp. 88–94. doi: 10.1061/(ASCE)HY.1943-7900.0000598.

Sherman, D. J., Davis, L. and Namikas, S. L. (2013) 'Sediments and Sediment Transport', in *Treatise on Geomorphology*. Elsevier Inc., pp. 233–256. doi: 10.1016/B978-0-12-374739-6.00013-0.

Shires, G. L. (2011) 'PECLET NUMBER', *A-to-Z Guide to Thermodynamics, Heat and Mass Transfer, and Fluids Engineering*. doi: 10.1615/ATOZ.P.PECLET_NUMBER.

Smith, E. H., Abumaizar, R. J. and Skipwith, W. (2001) 'Management of flood control sumps and pollutant transport', *Journal of the American Water Resources Association*, 37(1), pp. 17–25. doi: 10.1111/j.1752-1688.2001.tb05471.x.

Verbanck, M. A., Ashley, R. M. and Bachoc, A. (1994) ‘International workshop on origin, occurrence and behaviour of sediments in sewer systems: Summary of conclusions’, *Water Research*, 28(1), pp. 187–194. doi: 10.1016/0043-1354(94)90133-3.

APPENDIX A: PRELIMINARY EXPERIMENTAL DATA

***Table A-1**: Flow characteristic calculations (refer to **Equation 3-1**)*

Flow	Ha (m)	Bc (m)	Q (m^3/s)	Q (l/s)	θ (rad)	A(m^2)
Low	0.028	0.050	**3.07E-04**	**0.307**	2.705	1.46E-03
Med	0.043	0.051	**7.37E-04**	**0.737**	3.550	2.52E-03
High	0.068	0.011	**1.32E-03**	**1.315**	5.391	3.94E-03

***Table A-2**: Sediment characteristics*

Particle size (μm)	D_{50} (μm)	Density (kg/m^3)	Specific Gravity (SG)
150-300	124	2284	2.28
106-150	112.6	2186	2.19
75-106	76	2138	2.14

***Table A-3**: Kinetic power calculations*

Flow	P_{SUP} (W)	P_{hl} (W)	P_f (W)	P_{entry} (W)	P_{exit} (W)	$P_{W/O}$ (W)
Low	**6.78E-03**	0.12634	0.00073	0.00677	0.00337	**1.15E-01**
Medium	**3.15E-02**	0.30372	0.00314	0.03146	0.01569	**2.53E-01**
High	**6.55E-02**	0.48137	0.00642	0.06556	0.03278	**3.77E-01**

APPENDIX B: MASS-BALANCE READINGS

***Table B-1**: Mass-balance readings for Control setup (refer to **Equation 2-1**)*

TEST	FLOWRATE	SEDIMENT SIZE	m_i (g)	m_{outlet} (g)	m_{centre} (g)	m_{inlet} (g)	m_{total} (g)	$m_{w/o}$ (g)	η
1	LOW	COARSE	50	16.08	16.83	11.71	44.62	5.38	**0.8923**
2			100	13.61	34.89	32.75	81.24	18.76	**0.8124**
3			150	19.34	44.70	57.95	121.99	28.01	**0.8133**
4		MEDIUM	50	4.12	21.59	13.79	39.50	10.50	**0.7900**
5			100	9.95	37.11	36.50	83.56	16.44	**0.8356**
6			150	16.13	47.95	54.26	118.35	31.65	**0.7890**
7		FINE	50	3.38	16.76	20.64	40.78	9.22	**0.8155**
8			100	17.53	32.91	35.27	85.72	14.28	**0.8572**
9			150	13.09	53.03	54.61	120.73	29.27	**0.8049**
10	MEDIUM	COARSE	50	3.81	15.44	15.90	35.15	14.85	**0.7030**
11			100	7.25	29.38	30.26	66.89	33.11	**0.6689**
12			150	10.65	43.15	44.43	98.23	51.77	**0.6549**
13		MEDIUM	50	3.00	12.15	12.51	27.65	22.35	**0.5530**
14			100	6.23	25.25	26.00	57.48	42.52	**0.5748**
15			150	8.77	35.56	36.62	80.95	69.05	**0.5397**
16		FINE	50	2.77	11.24	11.58	25.59	24.41	**0.5118**
17			100	5.83	23.61	24.31	53.75	46.25	**0.5375**
18			150	8.09	32.78	33.76	74.63	75.37	**0.4975**
19	HIGH	COARSE	50	0.05	14.67	12.47	27.20	22.80	**0.5440**
20			100	0.42	27.91	21.50	49.82	50.18	**0.4982**
21			150	0.42	32.63	36.50	69.55	80.45	**0.4637**
22		MEDIUM	50	0.10	6.86	10.34	17.29	32.71	**0.3459**
23			100	0.21	16.75	18.60	35.56	64.44	**0.3556**
24			150	0.32	25.43	24.55	50.3	99.7	**0.3353**
25		FINE	50	0.13	6.96	6.83	13.92	36.08	**0.2785**
26			100	0.49	16.41	13.49	30.39	69.61	**0.3039**
27			150	0.51	16.20	21.86	38.57	111.43	**0.2571**

***Table B-2**: Mass-balance readings for Baffle Arrangement 1 (refer to **Equation 2-1**)*

TEST	FLOWRATE	SEDIMENT SIZE	mi (g)	m_{outlet} (g)	m_{centre} (g)	m_{inlet} (g)	m_{total} (g)	$m_{w/o}$ (g)	η
1	LOW	COARSE	50	16.49	10.56	19.74	46.79	3.21	**0.9357**
2			100	37.80	28.11	30.81	96.71	3.29	**0.9671**
3			150	50.55	49.85	47.31	147.71	2.29	**0.9848**
4		MEDIUM	50	16.60	12.27	19.31	48.18	1.82	**0.9635**
5			100	38.07	31.87	28.49	98.42	1.58	**0.9842**
6			150	43.38	51.85	51.99	147.22	2.78	**0.9814**
7		FINE	50	15.34	12.34	21.20	48.88	1.12	**0.9775**
8			100	38.94	25.92	33.92	98.78	1.22	**0.9878**
9			150	50.87	50.08	47.19	148.14	1.86	**0.9876**
10	MEDIUM	COARSE	50	20.71	14.14	9.59	44.44	5.56	**0.8888**
11			100	41.23	28.14	19.10	88.47	11.53	**0.8847**
12			150	61.61	42.06	28.55	132.22	17.78	**0.8815**
13		MEDIUM	50	20.37	13.91	9.44	43.71	6.29	**0.8742**
14			100	40.93	27.94	18.96	87.84	12.16	**0.8784**
15			150	60.69	41.44	28.12	130.25	19.75	**0.8683**
16		FINE	50	20.01	13.66	9.27	42.95	7.05	**0.8590**
17			100	39.99	27.30	18.53	85.82	14.18	**0.8582**
18			150	59.47	40.60	27.55	127.62	22.38	**0.8508**
19	HIGH	COARSE	50	22.87	17.79	0.04	40.70	9.30	**0.8140**
20			100	46.16	26.63	0.07	72.86	27.14	**0.7286**
21			150	70.60	33.81	0.10	104.51	45.49	**0.6967**
22		MEDIUM	50	19.97	9.70	0.10	29.77	20.23	**0.5953**
23			100	40.54	15.11	0.41	56.06	43.94	**0.5606**
24			150	51.27	24.39	0.71	76.37	73.63	**0.5091**
25		FINE	50	18.21	7.98	0.15	26.34	23.66	**0.5268**
26			100	31.80	14.50	0.64	46.94	53.06	**0.4694**
27			150	45.68	24.48	1.35	71.51	78.49	**0.4768**

***Table B-3**: Mass-balance readings for Baffle Arrangement 2 (refer to **Equation 2-1**)*

TEST	FLOWRATE	SEDIMENT SIZE	m_i (g)	m_{outlet} (g)	m_{centre} (g)	m_{inlet} (g)	m_{total} (g)	$m_{w/o}$ (g)	η
1	LOW	COARSE	50	21.41	15.41	11.31	48.12	1.88	**0.9625**
2			100	33.46	38.02	25.99	97.47	2.53	**0.9747**
3			150	45.93	53.30	48.30	147.53	2.47	**0.9835**
4		MEDIUM	50	18.77	16.76	12.68	48.21	1.79	**0.9642**
5			100	33.22	31.06	33.41	97.69	2.31	**0.9769**
6			150	54.72	43.30	49.33	147.35	2.65	**0.9823**
7		FINE	50	17.18	13.75	17.16	48.09	1.91	**0.9618**
8			100	30.68	33.24	34.96	98.88	1.12	**0.9888**
9			150	45.02	44.96	55.94	145.92	4.08	**0.9728**
10	MEDIUM	COARSE	50	15.21	14.83	14.56	44.60	5.40	**0.8920**
11			100	30.22	29.47	28.93	88.62	11.38	**0.8862**
12			150	45.25	44.12	43.32	132.69	17.31	**0.8846**
13		MEDIUM	50	14.09	13.73	13.48	41.30	8.70	**0.8260**
14			100	27.92	27.22	26.72	81.86	18.14	**0.8186**
15			150	41.89	40.84	40.10	122.83	27.17	**0.8189**
16		FINE	50	14.05	13.70	13.45	41.21	8.79	**0.8242**
17			100	27.43	26.75	26.26	80.44	19.56	**0.8044**
18			150	41.08	40.05	39.32	120.46	29.54	**0.8031**
19	HIGH	COARSE	50	13.79	13.75	16.13	43.67	6.33	**0.8735**
20			100	32.50	24.44	29.22	86.15	13.85	**0.8615**
21			150	46.60	42.77	41.52	130.89	19.11	**0.8726**
22		MEDIUM	50	9.08	13.21	16.83	39.11	10.89	**0.7823**
23			100	29.61	26.57	21.34	77.52	22.48	**0.7752**
24			150	39.80	38.82	40.24	118.87	31.13	**0.7924**
25		FINE	50	13.57	13.80	11.99	39.36	10.64	**0.7871**
26			100	23.05	26.05	27.13	76.23	23.77	**0.7623**
27			150	38.25	43.70	29.72	111.67	38.33	**0.7445**

***Table B-4**: Mass-balance readings for Baffle Arrangement 3 (refer to **Equation 2-1**)*

TEST	FLOWRATE	SEDIMENT SIZE	m_i (g)	m_{outlet} (g)	m_{centre} (g)	m_{inlet} (g)	m_{total} (g)	$m_{w/o}$ (g)	η
1	LOW	COARSE	50	19.05	18.38	10.68	48.11	1.89	**0.9621**
2			100	38.52	30.67	28.86	98.05	1.95	**0.9805**
3			150	58.58	48.29	39.00	145.86	4.14	**0.9724**
4		MEDIUM	50	20.54	17.57	10.22	48.33	1.67	**0.9665**
5			100	40.87	27.08	30.35	98.30	1.70	**0.9830**
6			150	58.58	48.29	39.00	145.86	4.14	**0.9724**
7		FINE	50	16.24	17.20	15.72	49.15	0.85	**0.9830**
8			100	32.83	30.11	36.26	99.19	0.81	**0.9919**
9			150	55.33	46.23	46.66	148.22	1.78	**0.9881**
10	MEDIUM	COARSE	50	18.25	15.25	15.39	48.89	1.11	**0.9778**
11			100	36.79	30.74	31.02	98.55	1.45	**0.9855**
12			150	54.96	45.93	46.35	147.23	2.77	**0.9815**
13		MEDIUM	50	18.12	15.14	15.28	48.54	1.46	**0.9708**
14			100	36.44	30.45	30.73	97.63	2.37	**0.9763**
15			150	54.74	45.75	46.17	146.65	3.35	**0.9777**
16		FINE	50	18.03	15.07	15.20	48.30	1.70	**0.9660**
17			100	36.40	30.42	30.70	97.52	2.48	**0.9752**
18			150	54.55	45.58	46.00	146.13	3.87	**0.9742**
19	HIGH	COARSE	50	17.26	12.11	18.55	47.92	2.08	**0.9584**
20			100	36.14	27.74	33.66	97.54	2.46	**0.9754**
21			150	46.26	51.81	47.12	145.19	4.81	**0.9679**
22		MEDIUM	50	14.36	14.40	18.50	47.26	2.74	**0.9451**
23			100	36.56	25.93	33.02	95.51	4.49	**0.9551**
24			150	58.18	43.13	44.10	145.41	4.59	**0.9694**
25		FINE	50	18.92	12.04	16.85	47.81	2.19	**0.9563**
26			100	35.37	29.01	32.77	97.15	2.85	**0.9715**
27			150	49.90	46.13	49.82	145.85	4.15	**0.9724**

APPENDIX C: ADV TEST READINGS

***Table C-1**: Flow velocity readings for Control setup*

Cell	V_x (mm/s)	V_y (mm/s)	V_z (mm/s)
1A	-14.825	39.494	0.403
1B	8.716	52.273	38.815
1C	-12.827	81.950	39.454
1D	-13.223	71.535	-21.430
2A	-22.035	41.354	-3.038
2B	-2.972	66.970	47.240
2C	1.888	66.835	50.965
2D	-3.912	63.664	36.263
3A	-23.652	34.950	-1.935
3B	-13.880	41.645	25.169
3C	11.100	47.189	63.696
3D	8.707	19.313	81.626
4A	-79.716	41.918	-24.239
4B	-22.093	40.097	1.308
4C	21.595	20.677	77.997
4D	-33.804	29.230	48.774
5A	-48.737	-8.057	-89.918
5B	-49.816	15.206	0.870
5C	-23.089	-4.264	60.358
5D	-106.471	0.019	108.524
6A	-14.448	-6.891	-48.790
6B	-20.544	-6.548	-30.267
6C	-0.238	-24.383	29.388
6D	91.608	-34.239	79.336
7A	25.027	-99.071	-60.328
7B	21.780	-139.152	-20.300
7C	20.131	-73.821	38.783
7D	16.082	-49.479	38.352
JA	-2.766	-78.214	13.917
JB	-13.661	-90.892	56.691
JC	32.415	-95.107	56.678
JD	110.214	-93.139	58.622
KA	26.585	-107.323	-59.559
KB	79.356	-151.417	5.765
KC	63.334	-61.502	-23.243
KD	60.730	-56.934	17.226

***Table C-2**: Flow velocity readings for Baffle Arrangement 1*

Cell	V_x (mm/s)	V_y (mm/s)	V_z (mm/s)
1A	-14.993	67.235	-21.504
1B	-	-	-
1C	-	-	-
1D	17.698	86.997	39.342
2A	-27.011	23.551	-12.120
2B	-	-	-
2C	-	-	-
2D	50.055	96.703	-58.664
3A	-1.596	15.718	-4.287
3B	-	-	-
3C	-	-	-
3D	-	-	-
4A	12.802	9.720	20.714
4B	-	-	-
4C	-	-	-
4D	-	-	-
5A	-4.836	43.695	24.125
5B	-	-	-
5C	-	-	-
5D	-	-	-
6A	-9.314	78.963	77.065
6B	-0.993	111.824	96.005
6C	-	-	-
6D	-	-	-
7A	0.141	107.922	53.121
7B	13.954	129.284	78.082
7C	-	-	-
7D	-	-	-
JA	-23.200	74.751	14.209
JB	-23.324	99.501	-2.108
JC	-	-	-
JD	-	-	-
KA	10.427	72.620	18.756
KB	6.411	119.775	-5.875
KC	-	-	-
KD	-	-	-

***Table C-3**: Flow velocity readings for Baffle Arrangement 2*

Cell	V_x (mm/s)	V_y (mm/s)	V_z (mm/s)
1A	0.103	17.129	42.174
1B	-	-	-
1C	-	-	-
1D	1.123	113.527	31.161
2A	-4.539	22.344	-12.432
2B	-	-	-
2C	-	-	-
2D	17.811	92.344	-80.471
3A	-3.043	12.203	-38.940
3B	-	-	-
3C	-	-	-
3D	29.549	12.136	-31.197
4A	-18.171	15.856	-18.844
4B	-	-	-
4C	-	-	-
4D	6.975	-7.726	26.529
5A	0.615	18.258	-40.932
5B	-	-	-
5C	-	-	-
5D	1.199	52.764	-28.765
6A	-0.155	12.256	-25.662
6B	-	-	-
6C	-	-	-
6D	-16.264	67.190	-7.643
7A	0.078	175.343	55.116
7B	-	-	-
7C	-	-	-
7D	60.097	72.218	-6.066
JA	16.222	74.324	10.905
JB	-	-	-
JC	-	-	-
JD	-42.250	47.273	1.488
KA	5.609	57.921	10.373
KB	-	-	-
KC	-	-	-
KD	-49.912	31.291	-10.407

***Table C-4**: Flow velocity readings for Baffle Arrangement 3*

Cell	V_x (mm/s)	V_y (mm/s)	V_z (mm/s)
1A	-7.521	-36.403	-2.806
1B	1.345	14.915	-31.984
1C	20.724	88.604	-36.638
2A	-23.992	-65.241	7.513
2B	-11.196	215.302	-4.883
2C	31.300	80.054	8.726
3A	-8.120	-43.898	7.537
3B	-10.218	32.989	37.074
3C	18.564	144.396	-46.585
4A	-6.941	-4.023	19.643
4B	-1.180	14.575	37.415
4C	5.825	78.757	-32.913
5A	-6.719	7.165	-2.100
5B	2.571	2.487	24.408
5C	-18.745	59.449	-0.370
6A	-13.763	3.906	1.873
6B	0.595	-21.813	13.527
6C	-1.882	50.031	-21.384
7A	2.111	13.183	-8.225
7B	5.356	17.824	5.444
7C	31.727	49.437	-14.166
JA	10.527	3.684	-1.393
JB	16.822	16.662	14.653
JC	7.155	37.132	-25.868
KA	20.843	17.258	-29.530
KB	-8.501	45.870	14.230
KC	-16.900	37.433	-22.887

APPENDIX D: SEDIMENT TRANSPORT ANALYSIS

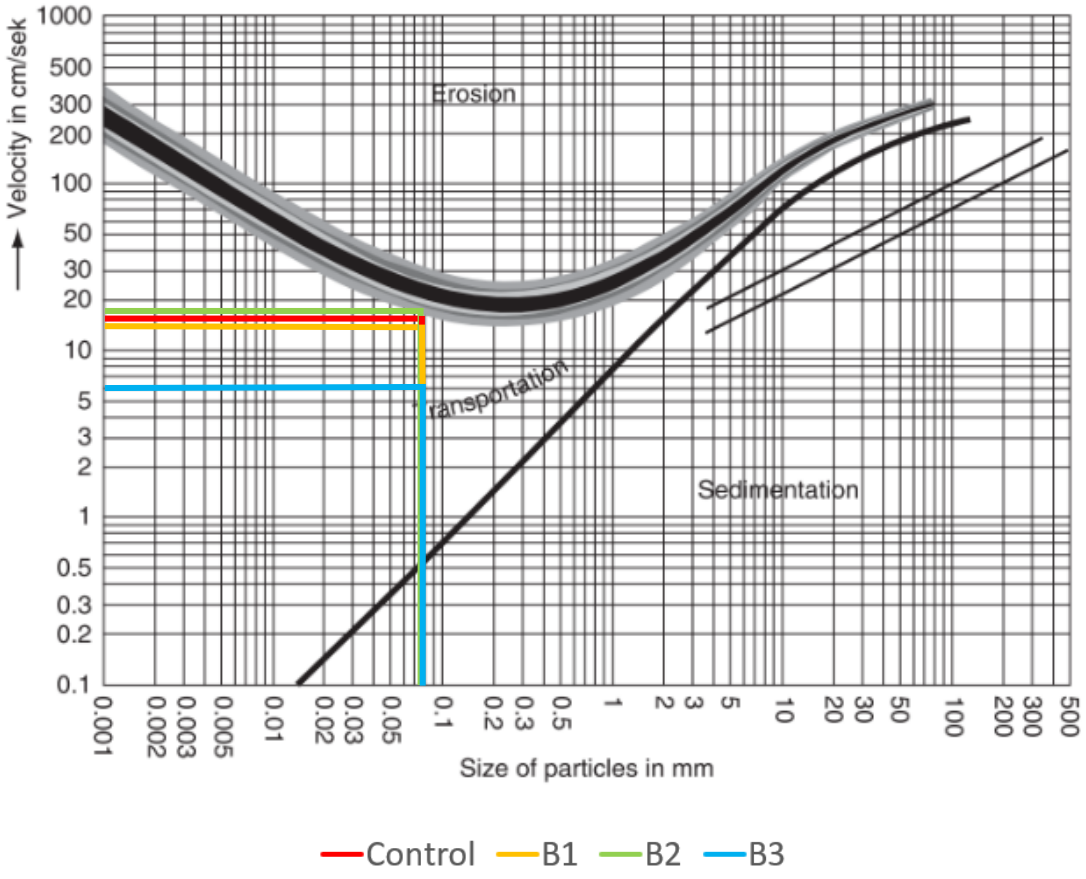

***Figure D-1**: Sediment transport analysis using Hjulström's Curve*

APPENDIX E: SCALING ANALYSIS READINGS

Table E-1**: Washout function values for all sump configurations (refer to **(Equation 2-2)

Uj (m/s)	Us (m/s)	Pe	Fr^2	Pe/Fr^2	C(SG-1)/(SG*ρw)			
					Control	B1	B2	B3
0.159	0.00706	5.72	0.0086	**665.70**	**3.17E-05**	**1.78E-08**	**1E-11**	**5.62E-15**
					4.29E-05	**2.41E-08**	**1.35E-11**	**7.59E-15**
					4.19E-05	**2.35E-08**	**1.32E-11**	**7.41E-15**
	0.00552	4.47		**520.34**	**3.03E-05**	**1.65E-08**	**8.94E-12**	**4.86E-15**
					3.91E-05	**2.12E-08**	**1.15E-11**	**6.27E-15**
					4.48E-05	**2.44E-08**	**1.32E-11**	**7.19E-15**
	0.00255	2.07		**240.56**	**3.23E-05**	**1.72E-08**	**9.17E-12**	**4.89E-15**
					1.89E-05	**1.01E-08**	**5.36E-12**	**2.85E-15**
					6.9E-05	**3.67E-08**	**1.96E-11**	**1.04E-14**
0.292	0.00706	1.13	0.0290	**39.11**	**9.14E-05**	**5.13E-08**	**2.88E-11**	**1.62E-14**
					1.93E-04	**1.08E-07**	**6.07E-11**	**3.41E-14**
					2.93E-04	**1.64E-07**	**9.23E-11**	**5.18E-14**
	0.00552	0.89		**30.57**	**1.47E-04**	**8E-08**	**4.35E-11**	**2.36E-14**
					3.07E-04	**1.67E-07**	**9.06E-11**	**4.92E-14**
					4.60E-04	**2.5E-07**	**1.36E-10**	**7.38E-14**
	0.00255	0.41		**14.13**	**1.49E-04**	**7.92E-08**	**4.22E-11**	**2.25E-14**
					3.31E-04	**1.76E-07**	**9.39E-11**	**5E-14**
					5.00E-04	**2.66E-07**	**1.42E-10**	**7.56E-14**
0.334	0.00706	0.64	0.0378	**16.83**	**1.07E-04**	**6.01E-08**	**3.37E-11**	**1.89E-14**
					2.34E-04	**1.32E-07**	**7.38E-11**	**4.15E-14**
					3.23E-04	**1.82E-07**	**1.02E-10**	**5.72E-14**
	0.00552	0.50		**13.15**	**1.84E-04**	**1E-07**	**5.44E-11**	**2.96E-14**
					3.80E-04	**2.07E-07**	**1.12E-10**	**6.1E-14**
					5.27E-04	**2.86E-07**	**1.56E-10**	**8.45E-14**
	0.00255	0.23		**6.08**	**1.80E-04**	**9.59E-08**	**5.11E-11**	**2.72E-14**
					4.02E-04	**2.14E-07**	**1.14E-10**	**6.08E-14**
					6.48E-04	**3.45E-07**	**1.84E-10**	**9.8E-14**